



TALLINNA TEHNIKAÜLIKOOL  
TALLINN UNIVERSITY OF TECHNOLOGY

Department of mechanical and industrial engineering

# DESIGN OF AN UNCONVENTIONAL QUADROTOR PROTOTYPE

EBAHARILIKU NELJAROOTORILISE MEHITAMATA ÕHUSÕIDUKI PROTOTÜÜBI  
DISAIN

MASTER'S THESIS

Student: Ott Tahk

Student code: 130377MATM

Supervisor: Martin Eerme PhD

Tallinn 2019

## AUTHOR'S DECLARATION

Hereby I declare, that I have written this thesis independently. No academic degree has been previously applied for based on this material. All works, major viewpoints and data of the other authors used in this thesis have been referenced.

May 27th 2019

Author:

.....  
*/ signature /*

Thesis is in accordance with terms and requirements

"....." ..... 20....

Supervisor:

.....  
*/ signature /*

Accepted for defence

"....." .....20... .

Chairman of theses defence commission:

.....  
*/ name and signature /*



# CONTENTS

- Preface..... 7
- Lists of used tables, figures and acronyms..... 8
  - List of tables ..... 8
  - List of figures ..... 8
  - List of acronyms..... 9
- Introduction..... 11
- 1. Literature overview ..... 13
  - 1.1. Lift creation and induced losses ..... 13
  - 1.2. Lift dissymmetry inherent to rotorcraft ..... 13
  - 1.3. Powering short distance flights ..... 15
  - 1.4. UAV designs..... 16
    - 1.4.1. Fixed wing platforms ..... 16
    - 1.4.2. Quadrotors ..... 16
    - 1.4.3. Helicopters..... 17
    - 1.4.4. Y4..... 17
  - 1.5. Control strategies ..... 19
- 2. Design of an improved Y4 prototype ..... 20
  - 2.1. Aim of the improved Y4 prototype..... 20
  - 2.2. Methods ..... 20
    - 2.2.1. Ecalc..... 20
    - 2.2.2. Computer aided design ..... 21
    - 2.2.3. Finite element analysis ..... 21
    - 2.2.4. 3D printing..... 22
  - 2.3. Design considerations ..... 23
  - 2.4. Selecting COTS hardware ..... 25
    - 2.4.1. Powertrain ..... 25
    - 2.4.2. Electronic speed controllers..... 26

|        |   |    |
|--------|---|----|
| 2.4.3. | Flight controller .....                           | 27 |
| 2.4.4. | Power distribution.....                           | 29 |
| 2.4.5. | Positioning .....                                 | 29 |
| 2.4.6. | Remote control.....                               | 29 |
| 2.4.7. | Battery .....                                     | 30 |
| 2.5.   | Designing the rotor head.....                     | 30 |
| 2.5.1. | Design considerations .....                       | 31 |
| 2.6.   | Designing the housings for electronics .....      | 41 |
| 2.7.   | Designing the frame components .....              | 43 |
| 2.8.   | Mass, balance and performance .....               | 46 |
| 2.8.1. | Masses.....                                       | 46 |
| 2.8.2. | Balance .....                                     | 48 |
| 2.8.3. | Performance.....                                  | 49 |
| 2.8.4. | Costs .....                                       | 50 |
| 2.9.   | Future directions and applications.....           | 52 |
|        | Summary .....                                     | 56 |
|        | Kokkuvõte.....                                    | 58 |
|        | References.....                                   | 60 |
|        | Graphics.....                                     | 64 |
|        | Y4 Drone assembly drawing 1:5; Sheet - A3.....    | 65 |
|        | Main motor assembly drawing 1:4; Sheet – A3 ..... | 66 |
|        | Teetering bracket drawing 1:1; Sheet – A4.....    | 67 |
|        | Rotor hub drawing 1:1; Sheet – A4 .....           | 68 |
|        | Blade holder drawing 1:1; Sheet – A4.....         | 69 |
|        | Fixing pin drawing 2:1; Sheet – A4 .....          | 70 |
|        | Teetering shaft drawing 2:1; Sheet – A4 .....     | 71 |
|        | Teetering spacer drawing 5:1; Sheet – A4.....     | 72 |
|        | Face plate drawing 2:1; Sheet – A4 .....          | 73 |

|  |    |
|--|----|
| Boom motor assembly drawing 1:4; Sheet – A4 .....              | 74 |
| Boom drawing 1:2; Sheet – A4 .....                             | 75 |
| Polypropylene 110mm pipe section drawing 1:2; Sheet – A4 ..... | 76 |
| Electronics stack assembly 1:2; Sheet – A3 .....               | 77 |

## PREFACE

In this thesis a quadrotor prototype with an unconventional Y4 layout, first proposed by Driessens and Pounds, is characterized and designed. The prototype is designed with a highly configurable main rotor enabling further research into this layout. The Y4 concept was selected because of the potential for large efficiency gains it would give and because of the complexity of its known problems and the unknowns of the configuration. The unorthodox layout promises up to 25% better efficiency than conventional quadcopters [1]. With this setup, a single large main rotor is producing the majority of lift and 3 rotors on booms extending from the body provide counter-torque and control. Although prototypes with this configuration have previously been assembled, a craft that would allow the direct comparison of different rotor head designs and control strategies has not yet been built. Therefore, this work gives a basis for further research and testing of this configuration.

This thesis was written to fulfill the graduation requirements of the Masters level study program Product development and Production Engineering in Tallinn University of Technology.

I would like to thank Pauline Pounds for her previous works and the help in answering my queries and my supervisor Martin Eerme for the support he gave. I would also like to thank my wife Siret Tahk for helpful comments and Janek Tauram for advice on machining.

Keywords: Drone, UAV, quadcopter, quadrotor, master's thesis.

# LISTS OF USED TABLES, FIGURES AND ACRONYMS

## List of tables

Table 2.1. Comparison of flight controllers..... 28

Table 2.2. Estimated masses of 3D printed parts..... 46

Table 2.3. Estimated mass of rotor head assembly ..... 47

Table 2.4. Masses of COTS components ..... 47

Table 2.5. Masses of other components ..... 48

Table 2.6. Costs of Y4 prototype components ..... 51

## List of figures

Figure 1.1 Dissymmetry of lift. .... 14

Figure 1.2. Y4 quadrotor's basic layout and control. .... 18

Figure 2.1. Generation and mitigation of lead-lag forces. .... 31

Figure 2.2. Rotor head assembly and section views of the rotor head mounted to the motor. .... 33

Figure 2.3. 2D static model of lift force acting on the blade and resulting reaction forces in the blade holder. .... 35

Figure 2.4. Thread strength simulation. .... 37

Figure 2.5. Load case for the rotor hub..... 38

Figure 2.6. Initial and refined rotor head design..... 39

Figure 2.7. Fixing pin minimum safety factor at design load, fully asymmetric lift. .... 40

Figure 2.8. Electronics stack ..... 41

Figure 2.9. Testing the ear plug mounting method..... 42

Figure 2.10. Upper Frame solid model and static stress simulation safety factor results. .... 43

Figure 2.11. Lower frame and static stress analysis results. .... 44

Figure 2.12. Boom motor mounts. .... 45

Figure 2.13. Landing gear PP-tube section and attachments..... 45

Figure 2.14. Experimental Y4 prototype – full CAD assembly ..... 49

Figure 2.15. Percentages of overall cost ..... 52

Figure 2.16. Possible test stand no. 1..... 53

Figure 2.17. Possible test stand no. 2..... 54

## List of acronyms

ASTM - American Society for Testing and Materials

CAD - computer aided design

CAN - controller area network

CEP - circular error probable

CNC - computer numerical control

CoM - center of mass

COTS - commercial off-the-shelf

CPU - central processing unit

CSI - camera serial interface

DDR3 - double data rate 3 synchronous dynamic random-access memory

EMI - electromagnetic interference

eMMC - embedded MultiMediaCard

ESC - electronic speed controller

FC - flight controller

FDM - fused deposition modeling

FEA - finite element analysis

FPU - floating-point unit

GB - gigabyte

GNSS - global navigation satellite system

GPIO - general purposed input-output

GPS - global positioning system

I2C - inter-integrated circuit serial bus

IMU - inertial measurement unit

LCD - liquid cristal display

MB - megabyte

PDB - power distribution board

PID - proportional, integral, derivative

PLA - polylactic acid

PP - polypropylene

PRU - programmable real-time unit

RAM - random access memory

KB - kilobait

RC - remote control

RPM - revolutions per minute

SBAS - space based augmentation system for GNSS

SBUS - Frsky inverted signal UART-like serial link

SPI - serial peripheral interface

UART - universal asynchronous receiver-transmitter

UAV - unmanned aerial vehicle

USB - universal serial bus

VTOL - vertical take-off and landing

Y4 - unconventional quadcopter configuration as proposed by Driessens and Pounds [[1](#)]

## INTRODUCTION

With ever increasing use of unmanned aerial vehicles (UAVs) for commercial and non-commercial applications, improving their energy efficiency needs to be addressed. The most popular layout for small scale vertical take-off and landing (VTOL) drones is the quadrotor configuration, which excels thanks to its mechanically simple construction.

Due to limited space and rotor flow interaction, there is a practical limit on the propeller size for each quadcopter platform and this makes them aerodynamically less efficient than a single main rotor helicopter configuration [34, 1]. Although single main rotor helicopter configurations have better aerodynamic efficiency than quadcopters, they are mechanically much more complicated having a multitude of moving parts for power transmission and rotor control. This makes them inherently less reliable, more costly to build and repair.

To address the growing pressure of minimizing the costs and improving the efficiency of VTOL UAV-s, this thesis sets out to aid the establishment of an alternative for the traditional modest-efficiency quadcopter configurations by providing an experimental Y4 quadrotor that allows further research into this simple, yet efficient configuration. The preliminary Y4 configuration was initially proposed by Driessens and Pounds and further expanded by Plessis and Pounds [1, 8]. It has one large fixed pitch main rotor to provide the majority of lift and three smaller rotors mounted on booms extending from the central frame to provide counter-torque and control. This solution is mechanically as simple as a quadrotor, but can be aerodynamically as efficient as a single rotor helicopter.

Previous work on the Y4 has been only partially successful [1, 8] and unanswered questions to its controllability, stability and performance are still present. Y4 with a fully rigid main rotor has not yet been successfully stabilized without significant gyroscopic effects and a teetering main rotor variant constructed by Driessens and Pounds exhibited fairly large tracking error from level trim. The reasons, why fully rigid prototype was not successful are unknown and direct comparison between rigid and teetering setups has not been done yet [1, 8]. In this thesis, a Y4 prototype with a novel highly configurable rotor head is designed. Combined with good processing power, excellent real-time performance and high-speed links between control electronics, this allows further research into the control dynamics of Y4 layout and the direct comparison of teetering and fully rigid rotor setups.

This thesis lays a solid groundwork to investigate the Y4 configuration further in terms of finding a successful control strategy for the fully rigid setup and experimentally determining the best configuration of rotor head, boom length, and boom motor cant angle. Then, full characterization of its flight envelope is possible.

The first chapter introduces the theory behind the aspects of this thesis and second chapter describes the design process in detail. When devising the prototype, initial estimations were done using the online multirotor design tool XcopterCalc and commercial off-the-shelf components were selected. The Y4 prototype was modelled and finite element analysis (FEA) run on Autodesk Fusion 360. In the later part of the 2<sup>nd</sup> chapter, mass and performance calculations are done. Masses for 3D printed components were estimated with IdeaMaker software and G-code was generated with RepetierHost. Lastly, the future directions were discussed.

Gaining more insight into the limitations and design aspects of Y4 configuration could enable the large-scale commercial adoption of this layout and realize the large efficiency gains promised. This could lessen the environmental impact of widespread usage of VTOL drones.

# 1. LITERATURE OVERVIEW

## 1.1. Lift creation and induced losses

The principle of any heavier than air vehicle flying is in accelerating air downwards to stay aloft. The most common ways of achieving this acceleration is to use wings or rotors. Both, wings and rotors, are airfoils which must move relative to air to deflect it down due to their geometry. Kutta–Joukowski theorem requires there to be a circulation around an airfoil, which is superimposed on the translational flow. This circulation is known as Kutta condition and it explains why the airflow on the upper surface is significantly faster than on the lower surface. According to Bernoulli's principle this difference in flow speeds will create a static pressure difference on the upper and lower surfaces [2].

Since all real-world lifting surfaces have a finite span, the pressure gradient will force air to flow over the tip of the lifting surface from high pressure side towards low pressure side creating a vortex. This flow over the tip of a lifting surface is called induced flow and it has an overall effect of tilting the total aerodynamic force vector further aft thus adding to the drag and reducing efficiency. To combat this effect, some airplanes have additional vertical surfaces at the wingtips called winglets [11]. Some designs place propellers at the wing tips which create opposing vortices to limit the effect of induced flow [12]. The load factor and pressure distribution on a lifting surface also play an important role in the creation of induced drag. If the pressure distribution across the length of a planar lifting surface is elliptical, the induced loss is at minimum [11]. Higher load factor necessitates greater pressure differential between upper and lower parts of the lifting surface, thus increasing the induced flow and its associated losses. Lower load factor is achieved though higher wingspan, which applies to propellers and rotors as well – the greater the diameter of a rotor producing a unit thrust, the lower the induced losses. For this reason, traditional helicopter designs with large main rotors enjoy less induced loss and hence better hover efficiency. [15]

## 1.2. Lift dissymmetry inherent to rotorcraft

When a lifting rotor has a horizontal velocity with respect to air, the side of the rotor which is rotating against the relative wind - advancing side experiences air velocity which is equal to the blade section's tangential velocity plus the velocity of the relative wind. A similar phenomenon happens on the side

which is rotating away from the wind - retreating side. The velocity across the blade section is equal to blade section's tangential velocity minus the velocity of the relative wind. This means the advancing side will encounter faster flow and retreating side will encounter slower flow. Since lift is proportional to velocity squared and the difference in speed between advancing and retreating side will grow with increasing forward speed, the dissymmetry of lift which will get ever worse with increasing speed. [14]

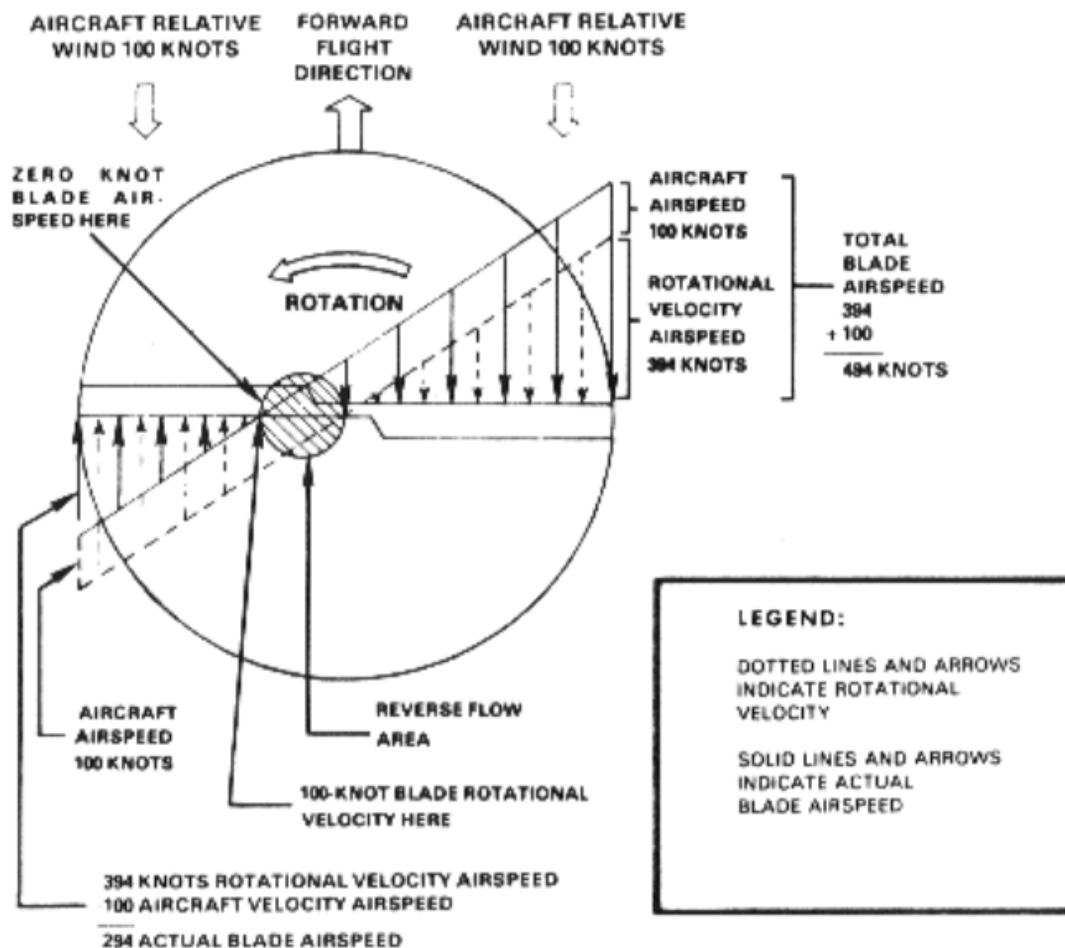


Figure 1.1 Dissymmetry of lift.  
 Source: Helicopter aerodynamics. Cantrell, P. [14]

Traditional quadcopters use counterrotating rotors in a symmetrical configuration so the dissymmetry of lift does not constitute a problem. Traditional helicopters tackle the problem by cyclically reducing the angle of attack on the advancing side and increasing it on the retreating side, so the center of thrust will always be at the hub. This can be done via one or a combination of the following: teetering hinge, flapping hinges, feathering hinges and blade flexing [14].

The problem of lift dissymmetry was also faced by the pioneer of rotary wing design - Juan de la Cierva in early 1920s. Then, the problem was solved by using flapping hinges to allow the blades to flap up on the advancing side and flap down on the retreating side effectively balancing out the lift being

generated on either side [13]. This shows that teetering or flapping hinges are a proven way of combating dissymmetry of lift at low speeds. There are also other ways of achieving balanced flight in conditions where high lift dissymmetry is expected. Winged lift compounding is one such method [44].

### 1.3. Powering short distance flights

The use of UAV-s for a variety of commercial applications, such as parcel delivery, various monitoring applications and as *ad hoc* relay stations has already become a widespread notion with a growing interest and big commercial impact. With large scale use of UAV-s, it is important to work towards lowering their associated greenhouse gas emissions for sustainable future. For short distance operations, it has been estimated that small-scale multirotor drones have lower life cycle greenhouse gas emissions than current ground transport options. Nevertheless, these results are heavily influenced by the methods of producing electricity and the efficiency and range of multirotor UAV-s, so working towards renewable energy production and better efficiencies is paramount [41].

Battery powered multicopters provide a more sustainable option for short range operations and urban environments than internal combustion powered counterparts due to geographically offset or lower overall pollution and reduced noise. Battery powered multicopters are well suited for short range operations and urban scenarios due to their vertical take-off and landing (VTOL) capability [41]. Battery powered drones are also mechanically much simpler due to the low count of moving parts and the ease of accurately controlling the speed of electric motors, but they lack the long range and endurance needed in some situations [45].

For long range or long endurance operations, fixed wing platforms offer much better aerodynamic efficiency. The fuels for internal combustion engines are also much more energy dense than the best batteries, making their use preferential in situations where long distances need to be covered or lengthy flight times are needed [45].

Battery powered drones are mostly limited in range due to low energy densities of batteries. Although, the industry is making progress in increasing energy densities of batteries, the aerodynamic efficiency of multicopters also needs improvement. The limitation of low energy density of batteries is still weighed down by the cheaper construction, low-noise operation and offset pollution of electric drones in urban environments and applications where long flights are not needed. Improved efficiency allows lowering greenhouse gas emissions and increase the range and payload capability of short range multicopter platforms [41].

## 1.4. UAV designs

### 1.4.1. Fixed wing platforms

Fixed wing platforms require the entire aircraft to be moving with a safe speed above stall speed relative to air, if they only rely on wings to provide lift. Wings have usually larger lifting surfaces when compared to rotary wing platforms, so while providing the same amount of lift required to keep the vehicle aloft, the pressure differences are not as large between the lower and upper surfaces leading to relatively low induced losses. Furthermore, airplanes do not have speed restrictions arising directly from the nature of their lift generation method, unlike helicopters [35].

Fixed wing aircraft have generally much better energy efficiency, can fly further and faster than rotary wing counterparts. What they are generally not good at is low airspeed maneuvering, vertical take-offs and vertical landings. Although, there are many hybrid designs like tiltrotors, tiltwings and tail-sitters, which can perform vertical take-offs and landings, airplanes generally require a runway or a complex mechanism to launch and retrieve them. Hybrid designs are usually also far from optimized for low speed tasks and suffer from lack of control authority due to low throttle margins in vertical flight and large vertical surfaces for the wind to act on. Additionally, the propellers used for vertical thrust are usually designed to provide thrust in forward flight and give low efficiency in low speed flight due to high disk loadings [35].

### 1.4.2. Quadrotors

There are many successful configurations of multirotors, including quadrotors, hexacopters, tricopters etc., but the most common and mechanically the simplest is the quadrotor. It uses only 4 actuators to control the aircraft. These actuators are its 4 motors and they enable control in all axes by just changing their speed. This makes them mechanically one of the simplest flying machines available. Mechanical simplicity usually leads to cheaper UAV-s, better reliability and lower maintenance costs [35].

The main shortcoming of quadrotors is their low efficiency due to high rotor disk loadings. Given a fixed footprint diameter, a quadrotor's rotor disks can only fill up an area of 4 circles inscribed by the bounding circle. In practice, this theoretical maximum is not used though, since flow interactions between the rotors will cause problems. A common rule of thumb is to leave a distance of  $\sqrt{2}$  times the rotor diameter between the rotors [34]. From this, it can be seen that a single rotor covering the entire footprint area would use the available space much better.

### 1.4.3. Helicopters

Helicopters use a given footprint quite well, since they usually have a large single main rotor. They have better efficiency than quadrotors, since they don't have to change the angular velocity of the rotor to change thrust and they do not have the low speed issues of fixed wing counterparts. Helicopters are much more easily scalable than quadrotors, since they usually have constant speed rotors. Changing the rotational speed of a rotor for control requires considerable energy to change the angular momentum and overcome the moment of inertia [36]. The moment of inertia scales with the 1<sup>st</sup> power of mass, which scales with volume – scale to the power of 3. Moment of inertia also scales with the square of the radius, so scaling a craft up by 2 increases the moment of inertia by 32 times (scaling factor to the power of 5) [37]. This is not a problem for helicopters, but it is for multirotors. Helicopters are well suited for low speed operations [35].

Helicopters have a number of problems, that make them less desirable in some applications. Firstly, they are inherently limited in speed due to retreating blade stall [14]. Secondly, they do not possess the efficiency, payload capability and speed of fixed wing aircraft, so they are limited to shorter range missions. The single main rotor construction also necessitates complex mechanical design to enable the cyclic and collective control of the main rotor's blades. This complexity increases the craft's initial cost, maintenance costs and makes it mechanically less reliable [35].

### 1.4.4. Y4

A novel quadcopter configuration was proposed by Driessens and Pounds [1] which offers the mechanical simplicity of a quadcopter while promising efficiencies similar to traditional helicopters. The design places a large fixed pitch rotor in the center of the fuselage which provides the majority of thrust to keep the craft flying. The large central rotor increases efficiency over traditional quadrotors due to its large span which decreases disk loading and decreases induced tip losses while occupying the same footprint as a quadrotor. The three smaller rotors - boom rotors are placed at the periphery to provide control and counter-torque. They are tilted from the plane of the main rotor to provide a horizontal component of thrust opposing the torque reaction created by the main rotor. The vertical component of thrust from these rotors is used to control the attitude of the craft. Control in all axes is achieved by this configuration while, like quadrotors, employing only 4 actuators (Fig. 1.2).

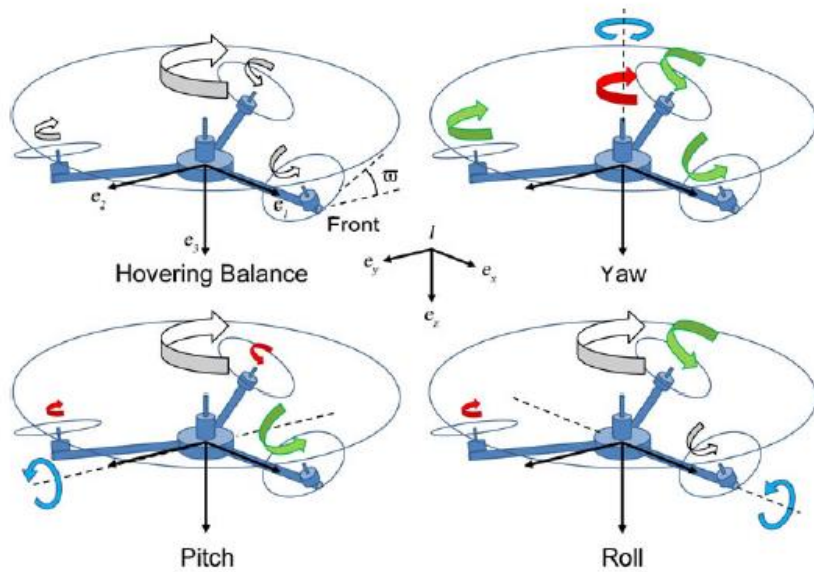


Figure 1.2. Y4 quadrotor's basic layout and control.

Arrow sizes and colors indicate rotor speed. White is constant, green is increased, red is decreased. Source: Driessens, Pounds. 2013 [1]

To provide yaw control, the main rotor is slowed down or sped up and simultaneously all the boom rotors are sped up or slowed down so the sum of vertical thrust produced by all rotors remains constant, but the torque reaction from the main rotor and the horizontal thrust components from boom rotors change, so yaw control is achieved. To provide pitch and roll control, the thrust from boom rotors is changed differentially keeping the torque created by horizontal thrust components equal to the torque reaction from the main rotor but creating a pitching or rolling moment.

The experimental fully rigid main rotor prototype of Driessens and Pounds experienced an uncontrolled precession in hover tests with a rotation of about  $2^\circ/\text{s}$  around yaw axis and an  $8^\circ$  pitch bias. The tests conducted by Driessens and Pounds did not reveal if the control problems were due to poor vibration isolation, bad boom motor placement or the control strategy selected. The tests also did not reveal the control bandwidth of the craft, but they showed that even without optimization and a slight disadvantage of rotor footprint, the Y4 was able to achieve 15% better hover efficiency than the control quadrotor. The theoretical maximum efficiency increase was shown to be 25% over a quadrotor with identical footprint [1].

The follow up to the work done by Driessens and Pounds was done by Plessis and Pounds and published in 2014. Using simulations, they showed that a fully rigid main rotor would be unstable under PID (proportional, integral, derivative) control with feedback linearization mainly due to control loop delays, but other control strategies were not explored. They showed experimentally, that a teetering hinge added to the main rotor would make the craft stable under PID control, but there were still unsolved problems. Their simulation results did not match well enough with the behavior observed in

experiments, there was a relatively large tracking error from level trim on the experimental teetering rotor craft and the PID gain values were not directly comparable with the results obtained by Driessens and Pounds due to different hardware used. The tests also did not exclude the viability of a fully rigid setup and they did not reveal data on high speed performance, where dissymmetry of lift would play a more prominent role [8].

## 1.5. Control strategies

PID control is the most common control strategy used in industrial engineering due to its simplicity. It is not the best solution for some control problems though. If there is considerable lag between control effort and response, if there are multiple variables to control simultaneously or if there is some planning required to keep the control variables within acceptable boundaries, PID may not be suitable [38]. Furthermore, in some applications, PID has been observed to produce large tracking errors similar to the one observed by Plessis and Pounds [39].

As Plessis and Pounds showed, control loop delay can play a major role in achieving stability [8]. Luckily, there are several strategies developed for non-linear systems with time delays. Hybrid control strategies show better characteristics in successfully stabilizing an underactuated multirotor in the presence of unpredictable disturbances and promise better robustness. They combine the strengths of simpler control strategies, but are harder to implement and usually computationally more demanding than simple PID [39]. Also, predictive feedback control has been shown to provide better results than PID in controlling non-linear systems with variable time delay with minimal increases in computational complexity [40].

## 2. DESIGN OF AN IMPROVED Y4 PROTOTYPE

### 2.1. Aim of the improved Y4 prototype

The goal of this thesis is to design a Y4 quadrotor prototype, which would enable further investigation of this configuration. The prototype would aid in answering the questions and solving the problems left unanswered by previous works on this design:

- Stabilization of fully rigid Y4 and implementation of a successful control strategy
- Establishing flight- and energetics characteristics of Y4 in high speed flight in fully rigid and teetering rotor configurations
- Establishing the effect of dissymmetry of lift on the craft
- Characterizing the design/mechanical factors affecting the stability of Y4
- Establishing a mission envelope best suited to Y4 configuration based on hover- and high-speed performance.

To enable these questions to be addressed, a prototype needs to be designed and built and well documented testing needs to be done. Finalizing the build, programming the flight controller and further testing are outside the scope of this work, but this work paves the way for them by designing the craft to allow for various comparative tests to be done on a single platform. A potential for 25% improvement in hover efficiency is a strong motivator to thoroughly investigate this interesting configuration.

### 2.2. Methods

#### 2.2.1. Ecalc

Initial sizing, cost estimation and motor selection decisions were done with the help of a multirotor design calculator called XcopterCalc on the Ecalc website<sup>1</sup>. The calculators and design tools provided by this site are considered the best available in the hobbyist segment and help to make quick design choices and component selections without wasting a lot of time searching the internet for what hardware manufacturers have on offer. This site contains a vast amount of data about various commercial off-the-shelf (COTS) drone components from most manufacturers.

---

<sup>1</sup> <https://www.ecalc.ch/>

### **2.2.2. Computer aided design**

The drone was modelled in Autodesk Fusion 360. Solid models for standard parts like nuts, bolts, threaded inserts etc. were imported in STEP format from McMaster Carr catalog. 3D assembly of the flight controller (FC) was downloaded from GrabCad (Beaglebone Blue, modeled by Elliott Wilson).

The COTS components that were modelled in computer aided design (CAD) software by the author were the following: main motor, main rotor blades, battery, power distribution boards, boom motors, electronic speed controllers (ESC), radio receiver module and boom propellers. User specified materials were created whose properties would match the materials intended to be used for making the parts. This enabled fairly accurate mass estimations of the parts and reasonably good static stress simulations to be done. Fusion 360 was chosen because it has good functionality and it is free for hobbyist users.

### **2.2.3. Finite element analysis**

Static stress finite element analysis (FEA) was done in Autodesk Fusion 360. All simulations were run using the linear static stress module in Fusion 360. Non-linear effects were reasoned to be not of interest, since stresses in the materials need to be below yield stresses. Initially, mesh was set to be coarse and simulations were run locally to get quick results and rectify problem areas before a more resource intensive simulation with finer mesh was run. It was seen that the tapered joint between main rotor blade holder and the rotor hub needs to have a much larger diameter than initially designed due to the large bending moments it has to withstand.

Mesh size was set to be 5% of model size. Also, local refinements were used, where previous iterations showed there were greater stresses. Cell sizes in local refinements were set as low as 0.5 mm. Fusion 360 defaults the contacts in assembly simulations to “Bonded” when generated automatically. Bonded surfaces are not allowed to move relative each other in any way during the simulation. Since bonded contacts do not represent the real world in many situations very accurately, as is when using bolted connections, the contacts were modified [\[27\]](#). Contact type “separation” was used in cases where sliding between surfaces was possible and a friction coefficient was defined based on the table from engineering toolbox website [\[22\]](#), bonded was only used between the washer and blade holder.

#### **2.2.4. 3D printing**

All parts that were designed to be 3D printed have been or will be printed using Tevo Tornado. Tevo Tornado is a fused deposition modeling (FDM) printer with single Bowden tube extruder. It is an improved clone of the original Creality CR-10. Its main features are a powerful heated bed running on 230V AC and a large build volume of 300 \* 300 \* 400 mm. A standard 0.4 mm nozzle is used.

Repetier Host running the popular Slic3r 3D slicer engine was used to create the G-code for the prints, because this slicer has consistently given good results in the past and the author has slicing profiles already tuned to the printer and filaments used. A layer height of 0.15 mm is used, because this has proven to give good surface quality even on near horizontal surfaces and fillets. Polylactic acid filament (PLA) is used for all 3D printed parts except for the teetering limiter, where polypropylene (PP) is used. PLA is one of the least temperamental filaments to print with and it has very good strength. Also, the material is one of the least expensive ones. PLA is not a material without compromises though. It softens at quite low temperatures. Depending on the specific blend, it can have a glass transition temperature of between 44°C and 63°C, which makes it not suitable for applications in environments with elevated temperatures. It can even noticeably soften when left in the summer sun. Furthermore, it will degrade with UV light and below its glass transition temperature it is one of the more brittle 3D printing materials [29]. Its low price and ease of printing still win out, since the experimental Y4 is only intended to be a research project, so longevity of materials is not a prime concern.

PP will be used for 3D printing the teetering limiter. Although it has a somewhat low tensile strength of around 32MPa, because of its exceptional toughness, fatigue resistance and good flexibility it was deemed to be the best material for absorbing energy when the main rotor tries to teeter beyond its designed maximum angle [30].

A bed temperature of 55°C, nozzle temperature of 205°C and a maximum speed of 100 mm/sec for the X and Y axis is used for the PLA. A bed temperature of 100°C, nozzle temperature of 220°C and a maximum speed of 25 mm/sec for X and Y axis is used for the PP. The best settings for PLA and PP have previously been tested. It was verified that low print speeds, high cooling fan settings and PP packing tape (or other bed adhesion improvement methods suited for PP) bed layer are needed to print good quality parts with PP. It has also been verified that PLA is compatible with high printing speeds, is not very temperamental in terms of bed adhesion and is able to be printed even without bed heating.

Bed adhesion must still be improved specific to each material used to get consistent results. The print bed on available Tevo Tornado is made of smooth glass which gives near polished surface finish to the first layer. A thin coat of hairspray solved in water is used to coat the bed with a sponge prior to printing. The bed is heated to printing temperature and water is let to evaporate. This gives a very thin layer of hairspray on the bed and ensures excellent adhesion for PLA. For PP, a layer of packaging tape is used on the print bed to ensure proper adhesion.

## 2.3. Design considerations

The design goals were set out to be following:

- Enable the comparison of teetering and rigid setups on same hardware;
- Enable the testing of different control strategies on same hardware;
- Enable the testing of different boom lengths and cant angles;
- All-up mass not over 2.5 kg;
- Main rotor diameter between 1 m and 0.5 m
- Use a design philosophy that would enable to:
  - 3D print as much parts as practical
  - use COTS parts where 3D printing is not practical
  - design rest of the components to be manufactured with a lathe, drill press, 3-axis milling machine and a 3-axis computer numerical control (CNC) router
- Thrust to weight ratio of at least 1.5
- Cost of 1000 € or less for all materials and COTS parts

As Plessis and Pounds have shown, control loop latency can play an important role in achieving a controllable Y4 [8]. Controllability with a fully rigid main rotor may even not be achievable, but to have the highest probability of success, stability control loop latency must be reduced to minimum. Control of the ESC-s must be achieved with the highest speed protocol possible on the selected hardware. Also, interpretation of sensor information and computing the desired control inputs must be done quickly enough to not be a bottleneck. Even with the lowest possible control loop times, some latency must be tolerated by the control strategy.

Time to send instructions to the ESC depends on the protocol used. One of the fastest protocols currently available is DShot1200, which is supported by BLHeli32 ECS-s. Ardupilot Copter 3.6 autopilot software and later editions support Dshot 1200, so Ardupilot will probably be the autopilot software used for the project. Another source of latency in the stability control loop will come from the inertial measurement unit (IMU) itself, so IMU sample rates are also an important factor in the design, so is the communication protocol used between the IMU and processor.

Low vibration levels for the IMU are needed to achieve good stability and attitude control. The most severe vibration in the Y4 design discussed in this paper is expected to be caused by imbalances in the main rotor. Since the main rotor is expected to operate mainly between 1000 and 3000 revolutions per minute (RPM), the vibration is assumed to be within the frequency band of 15-50 Hz. The boom

motors are also expected contribute due to slight mass imbalances, the boom flexing and aerodynamic interactions between the flow from the main rotor, the boom and the boom rotors. The main frequency of these vibrations is estimated to be in correlation with the boom motor's RPM.

To keep the unwanted vibrations to minimum, the construction of the frame and the booms needs to be as rigid as possible. Also, rotating parts need to be balanced as well as possible. The COTS motors are factory balanced, so further balancing effort in this respect is expected to be unnecessary. The rotors on the other hand are not factory balanced, so a rotor balancing stand will be used. Furthermore, a vertical through hole needs to be designed into the main rotor head for balancing purposes. The main rotor is expected to be the hardest thing to balance, since it will have the most sources of possible error. Additional holes drilled into the main rotor blades for rigid mounting add to the imbalance because small errors in the hole location will amplify due to large blade span. These imperfections must be offset by carefully balancing the main rotor system prior use and ensuring the center of mass of each blade will be coincident with the pitch change axis, so pitch changes will not affect the balance. During the first motor tests, it is expected that accelerometer data will show the prominent vibration frequencies making it possible to tune the vibration damping of the flight controller deck.

To find the best control strategy and to finetune the design, a number of parameters need to be measured, logged and analyzed. These are IMU data – rotations around and accelerations along all 3 axes, altitude, RPM and current consumption of each motor, battery voltage, speed and flight time.

Speed measurement will be accomplished with global positioning system (GPS) data, but wind speed during the tests needs to be accounted for. Battery voltage can be measured via some ESC-s using digital communication protocols or with a simple voltage divider voltage fed into the analog input of the flight controller. Current consumption of the motors can be digitally read via some ESC-s or voltage can be measured across a shunt resistor if all ESC-s are fed via a separate resistor. Motor RPM can be read with optical sensors, hall effect sensors or via some newer ESC-s. Measuring flight time should be relatively straight forward – all flight controllers and GPS sensors can provide time data that is accurate enough for the purposes of this project. Altitude can be measured with a barometer, radar altimeter, laser range finder or an ultrasonic range finder. Since barometric altimeter has the best range and is contained in most flight controller boards, this will be preferred.

All measured data should be stored on board or transmitted to some monitoring station. Since storing the data on board does not rely on a radio link, this is the preferred method. The flight controller would have to have enough excess storage space or have a micro SD card slot to achieve this.

Finally, a positioning system would need to be installed for high speed tests to get speed and position data and at least 4 channels are needed to be available on the remote control for controlling pitch, roll, yaw and power. More than 4 channels are preferable to give flexibility for future upgrades.

## 2.4. Selecting COTS hardware

### 2.4.1. Powertrain

The initial idea was to use the entire main rotor assembly of an existing 450 size remote control (RC) helicopter, similarly to Driessens and Pounds. Just attach the head to a motor, fix the blades and it's done. It was soon realized though, that achieving teetering, feathering, flapping or restricting lead-lag this way would be very difficult and hence the idea was judged to be impractical. A custom-made rotor head would offer much more flexibility.

The single most expensive item in a drone with design goals as stated in previous paragraph is the main motor. Therefore, starting the design process of the prototype with choosing the motor is reasonable. A quick search for available motors led to the conclusion that the first step should be choosing the battery voltage. This conclusion was made because smaller motors that would suite for boom motors are mostly designed to run on 4-cell LiPo-s or less. Larger motors that would turn the main rotor well are usually designed for higher voltages, from 6-cell up to 12-cell LiPo-s. A middle ground of 6-cell voltage (22.2 V nominal) was chosen because most main rotor candidates still run decently enough on 6-cell batteries and newer small racing drone motors are also 6-cell compatible. An online tool popular in hobbyist community – xcopterCalc from eCalc was used to choose the motors based on a 28-inch main rotor diameter (estimated to be roughly the right size to lift up to 1 kg of payload) and a rough estimate of the empty and maximum masses. A 130 Kv pancake style motor from MayTech was chosen (MTO-8626-130) because it was the cheapest motor that would have at least 800 W of power, good low speed torque, and decent 6-cell performance [20].

Align 28-inch (450 size) carbon fiber blades were chosen for initial testing for the main rotor because of their good availability, low weight, low price and reasonable stiffness. It is expected that these blades will be replaced rather soon after the design is experimentally validated and control software has been developed and tuned, since they are aerodynamically inferior to properly designed propellers. It is also not unreasonable to expect that these blades may be broken or get damage during testing. A proper carbon fiber propeller would be about an order of magnitude more expensive than these cheap blades but would offer little benefit in this early stage when control issues need to be

ironed out and efficiency is not paramount. These blades have a symmetrical NACA0013 profile and no twist.

The boom motors were chosen to be somewhat overpowered with an idea in mind to enable the investigation of controlled emergency landings in case of main rotor failure in the future and to give the craft plenty of control authority. Hobbywing Xrotor Race Pro 2207 1750 K<sub>v</sub> motors were chosen because of their excellent power to weight ratio, 6-cell compatibility, low price, good availability and reasonable efficiency.

For 2207 size 1750 K<sub>v</sub> motors it is generally recommended to use 5 – 7-inch propellers. Since these motors will run on 6S voltages and achieve higher RPM than on 4S, it was decided to use 3-bladed 5-inch propellers with a pitch of 4 inches.

#### **2.4.2. Electronic speed controllers**

When choosing the ESC-s, 2 goals were kept in mind – minimized latency and control flexibility. Low latency is desirable in most motion control situations, but especially in the control of a drone due to the high speed at which changes in position can occur. Furthermore, Plessis and Pounds showed, that the worse the control cycle latency was, the quicker the Y4 with rigid main rotor lost control under PID [8]. Although Plessis and Pounds showed that controlling a rigid main rotor Y4 under PID control is not possible, they did not rule out other control strategies [8]. Therefore, it was decided that there would be most chance of success with as fast a control loop as possible. Flexibility of controlling the ESC was also an important criterion. Since the author of this thesis was not familiar with the state of the art in RC prior to designing this experimental Y4, there were no strict criteria set for controlling the ESC-s. Equipment which allows the most flexibility in control would get a higher probability of getting selected.

Two different BLHeli32 ESC-s were chosen, CloudPhoenix Favourite 50A for the main motor and RCExplorer Aikon 35A for the boom motors. BLHeli32 ESC-s were chosen because they are compatible with DShot 1200 protocol – one of the fastest protocols currently available. The update rate of Dshot is 1200 bits/sek, which causes only about 13us of latency. BLHeli32 ESC-s are also capable of providing telemetry – current consumption, RPM, voltage and temperature. BLHeli32 supports current limiting, so there is less risk of overloading the ESC or the motor. With BLHeli32 ESC-s one can also set the maximum acceleration for the motor and send DShot commands to the ESC via flight controller. Currently only Multishot protocol can be faster than DShot 1200, but since the latency of Multishot depends on throttle setting, this is true only with low throttle settings. BLHeli32 enables the use of newest digital protocols, which gives constant update speed and plenty of flexibility [5].

### **2.4.3. Flight controller**

Keeping in mind the design considerations discussed previously, the main criteria for choosing the flight controller were:

- Large integrated storage volume or micro SD card slot
- Compatibility with Ardupilot, open source autopilot software
- Deterministic time computing capability for attitude control
- Have the needed connectivity to ESC-s
- Have reasonable computing performance
- Low price
- Flexibility for customization
- Contain an integrated IMU
- Have at least 5 analog inputs
- Have serial connectivity (universal asynchronous receiver-transmitter [UART], inter-integrated circuit serial bus [I2C], serial peripheral interface [SPI])

A table was composed for comparing the most popular flight control boards and choosing the best one for the experimental Y4.

| FC board                       | Processing   | Storage  | Baro-meter | IMU                      | Analog inputs | Connectivity  | Price (Eur) |
|--------------------------------|--|--|------------|--------------------------|---------------|---|-------------|
| Pixhawk                        | 168Mhz 32-bit ARM Cortex M4 + floating-point unit (FPU) 256 kilobait (KB) random access memory (RAM)   | 2 megabyte (MB) Flash  | yes        | 9-axis; redundant 6-axis | 8             | I2C, SPI, controller area network (CAN), UART, universal serial bus (USB), Frsky inverted signal UART-like serial link (SBUS) | 63          |
| Beaglebone Blue                | 1GHz ARM Cortex-A8; 2x32-bit 200-MHz programmable real-time units (PRU); 512MB double data rate 3 synchronous dynamic random access memory (DDR3) RAM; | 4 gigabyte (GB) embedded MultiMedia Card (eMMC); 32GB micro SD | yes        | 9-axis                   | 7             | I2C, SPI, CAN, UART, USB, WiFi, Bluetooth   | 71          |
| Erle PXF mini & Raspberry Pi 0 | 1GHz ARM 11; 512MB RAM   | Micro SD, no size limits                                       | yes        | 9-axis                   | 2             | I2C, UART, WiFi, Bluetooth, USB, camera serial interface (CSI), general purposed input-output (GPIO)                          | 100         |
| Navio 2 & Raspberry Pi 3       | 1.2GHz 64-bit quad-core ARMv8 central processing unit (CPU); 1GB RAM   | Micro SD no size limits  | yes        | 9-axis; redundant        | 2             | UART, I2C, SBUS   | 219         |

Table 2.1. Comparison of flight controllers.

The best fit for the criteria was Beaglebone Blue robotics controller board. It was chosen because it has good computing power, deterministic time computing capability and a lot of flexibility. It has 1 GHz main CPU, 512 MB of DDR3 RAM, 4 GB of on-board eMMC flash storage, two 200 MHz programmable real time units, integrated 9 axis IMU, many options for serial connectivity, 7 analog inputs for current monitoring or other analog sensing and it is compatible with Linux, ROS and Ardupilot [6, 7]. The main downsides of using Beaglebone Blue in this application are that it does not have an integrated GPS, its on-board gyroscopes have a sample rate of only up to 8 kHz and accelerometers have a sample rate of only up to 1 kHz and it does not have a redundant IMU like some other boards [9]. Redundancy was not considered important on an experimental platform, so this was not a major factor in deciding.

Plessis and Pounds [8] suggest that low control loop times are needed if the rigid main rotor setup is feasible at all, so 8 kHz gyro rate, 4 kHz accelerometer rate and an overall sample rate of up to 1 kHz

might mean the IMU can be the bottleneck of attitude control latency. Also, the Robotics control library made for the Beaglebone Blue does not have DShot compatibility yet to run the ESC-s on the newest protocol, using Dshot by other means is still possible though [10, 5]. Good processing power, fast PRU-s, relatively low price and many options for future improvements still led to choosing the Beaglebone Blue.

#### **2.4.4. Power distribution**

It was decided to power each ESC via a dedicated power distribution board (PDB). PDB selected for this project was the BabyPDB from RCExplorer. These PDB-s contain a shunt resistor for current measuring and a buck regulator for powering lower voltage loads. The buck regulator can be set to provide 12 V, 8 V, 6 V or 5 V via a solder joint. The buck regulator can provide up to 5 A on continuous current and up to 20 A of peak current.

The main reason for using 4 separate PDB-s is to provide a selection of lower voltages for the flight controller and its peripherals. Having 4 separate PDB-s would also provide back-up current monitoring capability for each motor in case there was an issue with getting Dshot to work on the flight controller. The chosen flight controller needs a 12 V supply, RC receiver needs 4 – 10 V, GPS receiver needs 3.3 V and any servos that could be installed for any reason in the future would need 6 V. These 4 boards have more than enough current handling to supply all loads.

#### **2.4.5. Positioning**

XA1110 Qwiic GPS breakout board from SparkFun was selected as the main positioning device. A single global navigation satellite system (GNSS) input will be enough for initial testing, but additional sensors like an optical flow sensor could be installed when probable control issues have been solved. The XA1110 has an onboard memory battery, which allows warm starts, so it is possible to get a position fix in just 5 seconds after turn on. It also features an update rate of 10 Hz, which is necessary to accurately position a fast-moving drone. The XA1110 has a positioning accuracy of 2.5 m when utilizing space-based augmentation systems (SBAS) with a circular error probable (CEP) of 50 % [23].

#### **2.4.6. Remote control**

FrSky ACCTS XSR full duplex telemetry receiver and FrSky Taranis X9D Plus remote control will be used with the experimental Y4. Taranis X9D Plus transmitter was selected because it has a very good set of features for the price, it has a wide user- and support base and it has a good reputation. The transmitter

has 16 channels, a big liquid crystal display (LCD) display and works on the 2.4 GHz band. The receiver has 16 channels, connects to the flight controller via an inverted UART serial protocol - SBUS or pulse position modulation [24]. Since the flight controller will not work with inverted UART signals directly, a signal inverter will need to be installed in line [25]. The transmitter-receiver combination chosen supports full duplex communication, so telemetry can be seen in near real time.

#### **2.4.7. Battery**

Maytech MTO-8626-130 is rated for maximum current draw of up to 32 A [20]. The boom motors can individually draw up to 39.75 A, so collective maximum is 119.25 A [26]. This means the maximum current draw from motors can be 151.25 A. Factoring in additional loads from the flight controller and other devices, a battery with at least 160 A current capability is needed. Although maximum currents can be limited with ESC-s and it is expected that boom motors would very rarely, if at all need full amperage at the same time, the good availability and power densities of LiPo batteries led to them being chosen.

A Zippy Compact 40 C 6200 mAh 6-cell LiPo battery was selected to power the craft. 6200 mAh battery was chosen because this is a reasonable size for a 2-3 kg drone. This battery can provide over 200 A of continuous current which is plenty for the selected motors. Zippy LiPo batteries have a good price point as well, so they are less costly to replace if damaged.

## **2.5. Designing the rotor head**

A main rotor head was designed that would allow for

- the freedom to teeter or conversely to lock the head from teetering
- easy adjustment of the blade pitch and possibility of locking the blades firmly in place
- lead-lag freedom for the blades or conversely locking that freedom if needed

The rotor head was designed to be machined using a lathe, drill press, a 3-axis milling machine and a 3-axis CNC router and be made of materials simple to acquire. The rotor head is the most critical and intricate part of the experimental Y4, so its design process is explained in more detail.

### 2.5.1. Design considerations

The easiest way to limit the lead-lag freedom would be to use two bolts to hold each blade in the blade holder. This way the lead-lag freedom can be allowed by just removing one bolt and locking the freedom would be achieved by installing it. Attaching the blades this way can introduce quite a lot of variability in the location of rotor's center of mass and cause unwanted vibrations. Once the blades are attached, the balance needs to be checked and adjusted. Then the attachment bolts need to be tightened, so friction keeps the blades in place. Since the blades are quite long, even small lateral loads on the blades get amplified by the arm and need to be accepted by the blade holders. It is needed to reduce any lateral loads that produce lead-lag moments.

One way of reducing lead-lag forces in a teetering rotor is to have the teetering axis coincident with the plane of blades' center of mass. This way, the lead-lag loads coming from tilting the rotor are kept symmetrical when the disk is loaded. Disk tilting causes lead-lag forces because the blades cone when they are producing lift and if the teetering axis is coincident with the rotational plane of the blades center of mass (CoM) in the unloaded state, then during coning this will not be so. When the disk is loaded and being tilted, the blade's center of mass is moving closer or further from the teetering axis and due to conservation of angular momentum, the blade wants to speed up or slow down. Because of this, it is needed to have the teetering axis above the blades' center of mass plane when disk is unloaded. This way, when blades are under load and flex, the rotational plane of blades' CoM approaches the teetering axis and any change of blade's CoM distance from the teetering axis will be symmetrical (Fig. 2.1) [17].

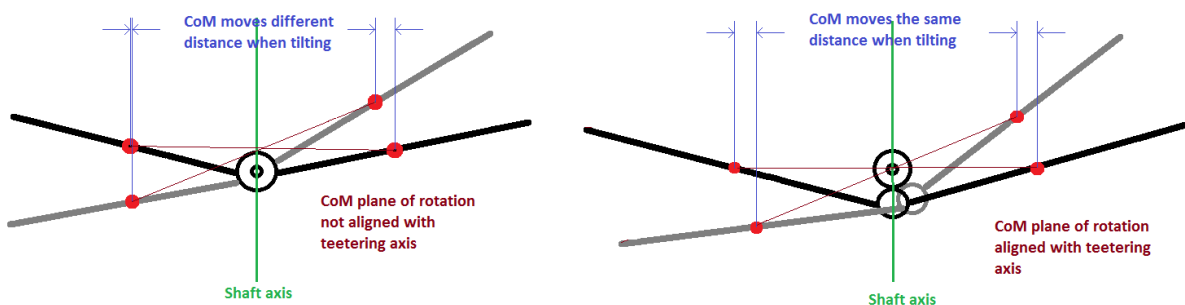


Figure 2.1. Generation and mitigation of lead-lag forces.

Left: regular rotor; Right: underslung rotor. Rotor in its tilted state is depicted with grey color. Coning and tilting is exaggerated.

Changing the pitch of the blades would have to be simple and the blade positioning as repeatable as possible. Using COTS 450 size RC helicopter rotor head was considered because it already has the necessary components to allow pitch change and to fix the pitch via pitch links if needed. Still, it was

concluded that using COTS RC helicopter rotor head would have considerable draw-backs and a custom solution would be needed. The limitations of using existing rotor heads were:

- Unknown strength and safety factor to accept the design loads
- Overly complex design for the Y4 application – pitch links, pitch bearings etc.
- No apparent way of allowing rotor teetering
- No robust way of fixing the lead-lag freedom

For these reasons, it was decided to design a bespoke rotor head for the Y4.

The idea on how to fix the pitch of the blades while allowing easy adjustment comes from machine spindles. Tapered spindle attachments create a strong connection with large contacting surfaces and create ample friction. They are also very repeatable and ensure good concentricity [31]. It was decided that a self releasing taper with slightly steeper included angle than on standard CNC spindles would be suitable. The taper needs to be steep because a steep taper will not keep the interference fit when the tensioning bolt is released enabling easy adjustment of blade pitch. The angle also needs to be steep to limit the transverse loads on the joint, so aluminum can be used as the material for blade holders and rotor hub. Bolt preload to hold the tapered joint needs to be quite high to counter the centrifugal forces from the rotor blades and still keep the joint tight, so most aluminum alloys would have stresses exceeding yield stress when keeping the rotor head dimensions acceptably small.

To allow the rotor to see-saw a teetering joint need to be designed. The joint must allow the rotor to teeter around the see-saw axis, but constrict all other translations and rotations. A teetering shaft running on 2 deep groove ball bearings will suffice for this, since translational forces along the shaft axis will be negligible. There also needs to be a way of reliably and repeatably fixing the teetering freedom. For this purpose, set screws, an additional fixing bracket and a fixing pin were considered. Using a fixing pin to lock the teetering freedom was deemed the best option due to its simplicity.

The designed rotor head assembly consists of:

- Bracket – attaches to the main motor's rotor with 4 M3 bolts and connects to the rotor hub via a teeter joint (teeter shaft, ball bearings, washers and end bolts). Aluminum 6082-T6
- Rotor hub – the part where blade holders attach to. Made out of aluminum 6082-T6.
- Blade holders – are connected to the hub via a 24° taper, preloaded with 3000 N of force and held in place with an American Society for Testing and Materials (ASTM) F568M class 12.9 (or equivalent) M4 bolt. Made out of aluminum 6082-T6.
- Teeter limiter – limits the free teetering of rotor head to 7.5° (similar to R44 helicopter [3]). 3D printed polypropylene.

- Fixing pin – can be installed right side up or up side down. If installed one way, helps center the bracket on the motor. If installed the other way, helps center the bracket on the motor and stops rotor head from teetering. Made out of medium carbon steel.
- Teetering joint – 5 mm shaft, M3 end bolts, washers, spacers and 5x10x4 mm ball bearings.
- M3 bolts for attaching teetering limiter to the bracket and the rotor head assembly to the motor. ASTM F568M class 8.8 bolts or equivalent.

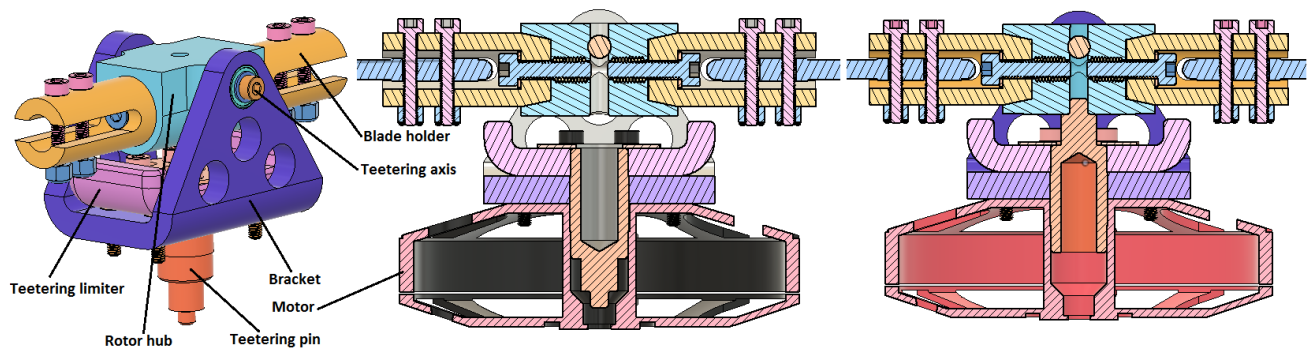


Figure 2.2. Rotor head assembly and section views of the rotor head mounted to the motor. Section view in the middle shows locking pin in neutral position, section on the right shows fixing pin locking the teetering freedom.

The teetering axis was designed to be 5 mm above the blades pitch axis because this would allow the blades center of mass to approach the teetering axis when the blades flex under load. This would keep the rotational plane which goes through the blades center of mass almost coincident with the teetering pivot point and reduce lead-lag forces [17].

Blade holders were designed to be held in place with a tapered joint and a single bolt (Fig. 2.2), because this kind of joint would be strong, compact, easy to loosen or tighten and repeatable. A taper angle of 24° was selected for the joint between the blade holder and rotor hub because it would be a self-loosening taper making it easy to adjust blade pitch.

Desired blade pitch can be set by measuring the angle between the plane cut into the blade holder and the horizontal plane milled on the rotor hub, adjusting as desired and tightening the M4 screw. Tapered connection will have more friction than the planar connection between bolt head and the blade holder due to the taper geometry amplifying the normal force and aluminum-aluminum contact having much greater coefficient of friction than that of a steel-aluminum contact [22]. Because of this, adjustments of blade angles should be quite straight forward.

The maximum angular velocity ( $\omega$ ) that the main motor can develop in its unloaded state is [4]

$$\omega = K_v * U, \tag{2.1}$$

where  $\omega$  – angular velocity, rad/s

$K_v$  – motor velocity constant, RPM/V,

U – peak voltage, V

The main motor chosen for the drone has a  $K_v$  of 130 RPM/V. Since the nominal voltage of the chosen battery is 22.2V we can assume the maximum  $\omega$  the motor will see is

$$\omega = 130 \text{ RPM/V} * 22.2 \text{ V} = 2886 \text{ RPM} = 302 \text{ rad/s}$$

The main rotor blades used on the initial prototype weigh 27.3 g, their maximum radius will be 365 mm and their innermost radius will be 26.5 mm. A simplifying assumption is that the blades are homogenous in their mass distribution and we can assume the center of mass radius ( $r$ ) to be located at the center of the blade as  $r = (365 \text{ mm} + 26.5 \text{ mm})/2 = 196 \text{ mm} = 0.196 \text{ m}$ .

It was also assumed that the next blades used on the same rotor head will be more complex and probably more massive, so a safe bet of maximum single rotor blade mass of 60 g was chosen for calculations based on half-mass of existing carbon fiber propellers [16].

The total force acting on the blade holder is a sum of the centripetal force on the blade, total aerodynamic force acting on the blade and apparent forces due to blade center of mass distance change from the rotation axis and the conservation of angular momentum. The centripetal force was estimated to be at least an order of magnitude larger than other forces, so it was calculated for first.

The estimated centripetal force ( $F_c$ ) the rotor head has to withstand with maximum  $\omega$  and blade mass is

$$F_c = m r \omega^2, \tag{2.2}$$

where  $F_c$  – centripetal force, N

$m$  – mass of rotor blade, kg

$r$  – radius of center of mass of the blade, m

$\omega$  – angular velocity, rad/s

Therefore, with a blade mass of 60 g, the centripetal force is

$$F_c = 0.06 \text{ kg} * 0.196 \text{ m} * (302 \text{ rad/s})^2 = 1073 \text{ N}$$

Based on this, a blade holder bolt preload of 3000 N opposing the centrifugal force and holding the taper joint together was estimated to be adequate.

According to the manufacturer, the main motor can produce up to 4.689 kg<sub>F</sub> of thrust [20]. Rounding that up to 50 N and dividing by 2, we get that 1 blade produces (F<sub>L</sub>) up to 25 N of thrust in normal operating conditions. The lift force acting on a blade (F<sub>L</sub>) is simplified to be a point force acting at 75% radius station. We can then solve the system statically, for the moment neglecting lead-lag and centripetal forces.

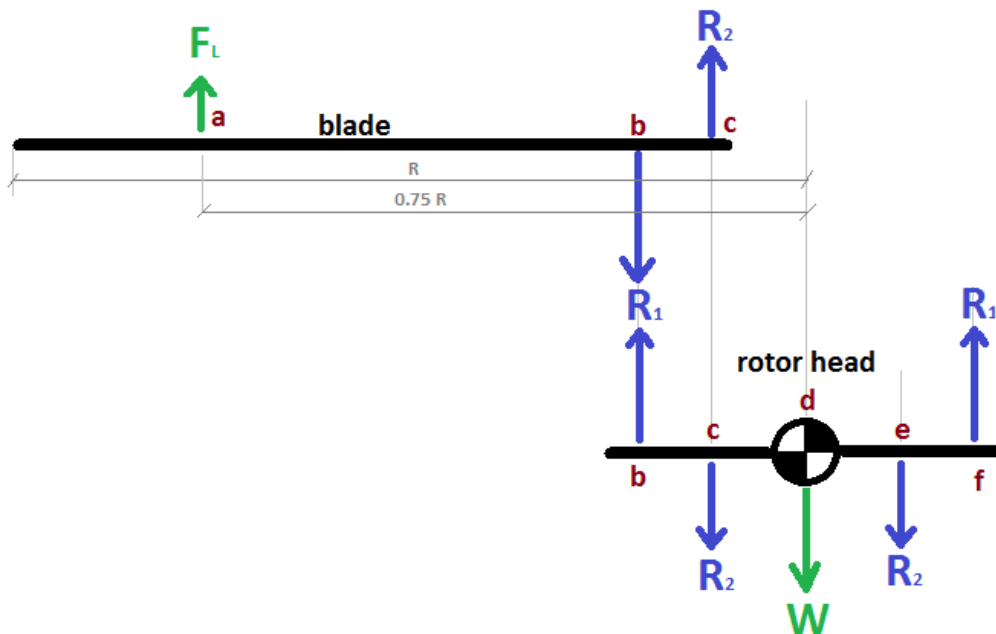


Figure 2.3. 2D static model of lift force acting on the blade and resulting reaction forces in the blade holder.

For a system to be static, the sum of all forces and moments at any point must be 0, therefore

$$F_L + R_2 - R_1 = 0 \Rightarrow R_1 = F_L + R_2 \Rightarrow R_2 = R_1 - F_L \quad (2.3)$$

where  $F_L$  – lift force acting on the blade, N

$R_1$  and  $R_2$  – reaction forces at blade attachment points, N

and

$$M_b = 0 \Rightarrow (R_2 * D_{b-c}) - (F_L * D_{a-b}) = 0, \quad (2.4)$$

where  $M_b$  – sum of moments in point b, N\*m (see Fig. 2.3)

$R_2$  – reaction force in point c, N (see Fig. 2.3)

$D_{b-c}$  – distance between points b and c, m (see Fig. 2.3)

$D_{a-b}$  – Distance between points a and b, m (see Fig. 2.3)

Now we have a linear system with 2 unknown variables, so equations 2.3 and 2.4 can be rearranged as

$$((R_1 - F_L) * D_{b-c}) - (F_L * D_{a-b}) = 0 \Rightarrow R_1 = ((F_L * D_{a-b}) / D_{b-c}) + F_L, \quad (2.5)$$

From the CAD model we know that the main rotor radius  $R = 0.365$  m.

The radius of 75% station is  $D_{a-d} = R * 0.75 = 0.365 \text{ m} * 0.75 = 0.274$  m.

Also, from the CAD model we know that distance  $D_{c-d} = 0.0365$  m and distance  $D_{b-c} = 0.008$  m, thus distance  $D_{a-b} = D_{a-d} - D_{b-c} - D_{c-d} = 0.274 \text{ m} - 0.0365 \text{ m} - 0.008 \text{ m} = 0.2295$  m

Using equation 2.5, we see that  $R_1 = ((25 \text{ N} * 0.2295 \text{ m}) / 0.008 \text{ m}) + 25 \text{ N} = 742 \text{ N}$

Using equation 2.3, we see that  $R_2 = R_1 - F_L = 742 \text{ N} - 25 \text{ N} = 717 \text{ N}$

Carbon fiber blades designed for this size category will handle these loads easily, but rotor head would have to be checked with FEA static load analysis with these loads. Three different simulations were run to find out the strength of inner threads in the rotor hub, the safety factor of blade holder and rotor hub under design loads and the safety factor of the fixing pin under design loads. A minimum safety factor of 2 was set as the design goal for the blade holder tapered joint and the bolt joint and 1.5 for the fixing pin in the worst-case load situation. Fixing pin has a lower safety factor, since its failure would most probably not bring the drone down and the worst case design load is not expected to occur in the flight tests, since it is highly improbable, that the drone would be capable of reaching speeds that produce a fully asymmetric load condition – the magnitude of UAV's forward speed equaling the absolute value of tangential velocity of retreating blade's tip section.

First, a static load simulation was run on Fusion 360 to find out if the inner threads cut into the rotor hub would be able to withstand the required preload. For a bolt joint, the end goal was not to reach a safety factor of 2 in the FEA simulation, since the largest stresses in the joint would be due to bolt preload and any surface imperfections in the threads will probably yield for compliance. The preferred end goal was that the bolt strength would be at least twice the preload value and that it would break before the inner threads if the design loads were exceeded.

A single M4 screw was selected to retain the blade holder in the tapered socket of the rotor hub. Recommended maximum tightening torque for M4 screws is around 5 Nm depending on the screw material, housing material and friction [18]. The resulting axial preload from 5Nm of torque with friction coefficient of 0.2 is over 6000 N [19]. The proof load for ASTM F568M class 12.9 M4 size bolt is 8520 N [20], so if the sum of bolt preload and centrifugal forces are below half of that value and it is ensured that the bolt is the weakest link, then a safety factor of 2 is ensured.

Since the blade centrifugal forces oppose the bolt preload, this means the preload must be larger than the centrifugal force with a reasonable margin. A preload of 3000 N and M4 bolt size were considered to be adequate and well within the capabilities of a M4 bolt. Also, combined load on the bolt would be  $3000 + 1073 = 4073$  N, which is less than half of the proof load of a class 12.9 bolt.

A simulated bolt connection with 3000 N of preload and a bolt head washer was used for the FEA simulation. The FEA showed that if the internal threads were to be cut into 6082 T6 aluminum with an effective length of threaded hole of 9.5 mm for each bolt, the resulting threads would have marginal capability of reliably holding the bolt under design loads. Furthermore, the internal threads would probably be the first to rip in an overload situation (Fig. 2.4). It was decided that a SAE 304 stainless steel threaded insert was best added to the design and a FEA was run again. Although the threaded insert shortens the effective threaded length from 9.5 mm to 8 mm, the material is much stronger than aluminum and also does not wear as fast when the blade pitch is often adjusted. Also, second simulation showed the weakest part to be the bolt which was the intended goal.

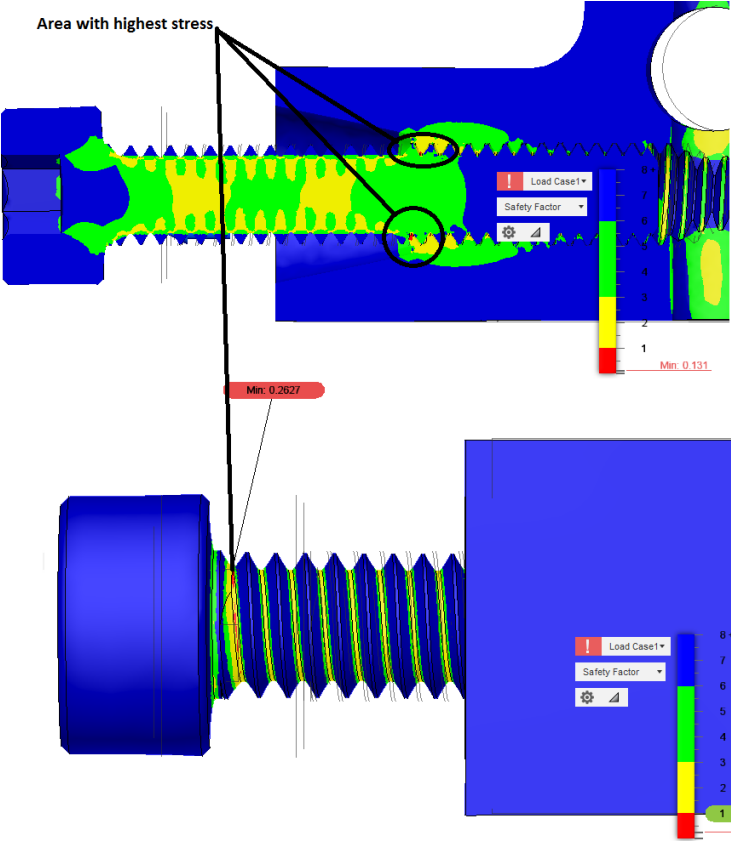


Figure 2.4. Thread strength simulation. The 1. result is for threads cut into aluminum and show the weakest point to be the inner threads closest to the bolt head. The 2. result is with stainless steel threaded insert and shows the bolt to be the weakest part.

Next, a static load FEA simulation was run on Fusion 360 to estimate the safety factor of the rotor blade holders and the rotor hub under design loads. Aluminum 6082 T6 was used as the study material again for both, the rotor hub and the blade holders. 6082 T6 aluminum is widely available in many profiles including round, square and rectangular stock in many dimensions. The material has good strength and is easily machinable and due to aluminum’s low density will give lower mass parts in many applications when compared to steel. Material properties were inserted manually to Fusion 360 from Matweb materials database website<sup>2</sup>.

The model was simplified for the simulation by splitting the rotor hub in two and only simulating one half of the rotor system. A further simplification was that the blade holder was cut shorter since the main interest was in the tapered joint and the bolt joint and previous coarse mesh simulations showed that the blade attachment part of the blade holder does not receive loads that would be approaching yielding point of the material.

A point mass simulating the rotor blade was placed 196 mm from the center of rotation and attached to the outermost face of the blade holder. An angular rate of 302 rad/s was defined for the study assembly around the rotation axis. A remote (offset) force of 25 N was placed 274 mm from the rotation axis and set acting on the blade holder. This force simulates the lift generated by the blade and it was set to be half of maximum thrust expected from the rotor. A rigid constraint (in all 3 axes) was put on the surfaces created by splitting the rotor hub, since this is the plane of symmetry. Gravity was turned on for the simulation and finally a simulated bolt connection with a preload of 3000 N was used (Fig. 2.5). A general mesh size of between 1 and 3 % of the model size was used. Highly stressed areas were locally refined with 0.1 – 0.3 mm maximum cell size depending on the size of the feature in interest. All simulations were run on cloud.

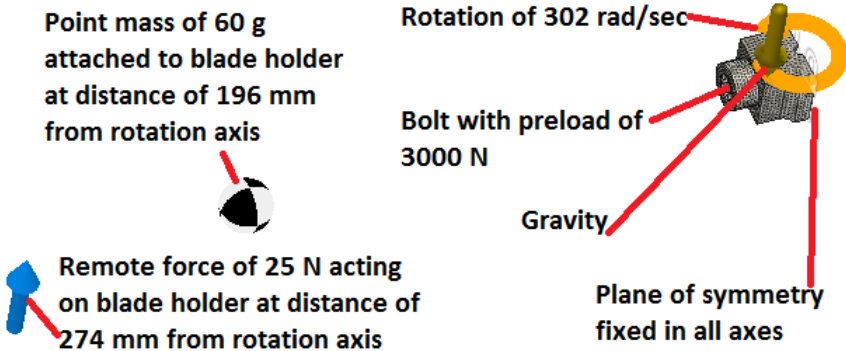


Figure 2.5. Load case for the rotor hub.

<sup>2</sup> [www.matweb.com](http://www.matweb.com)

When simulating with assemblies, contacts defined between the bodies play an important role. Contact in the tapered joint and the contact surface between bolt head and blade holder were defined as “separation”. In Fusion 360 this means the surfaces can not penetrate each other but can separate and slide. For realistic simulation of sliding, a friction coefficient of 1.2 was set for aluminum to aluminum contact and 0.61 for aluminum to steel contact [18].

The simulations showed that there would be yielding in the initial design of the blade holder – in the tapered joint of the rotor hub and in the blade holder under the bolt head, so the dimensions of the taper were increased and a steel washer was added under the bolt head to increase the effective surface area (Fig 2.6.).

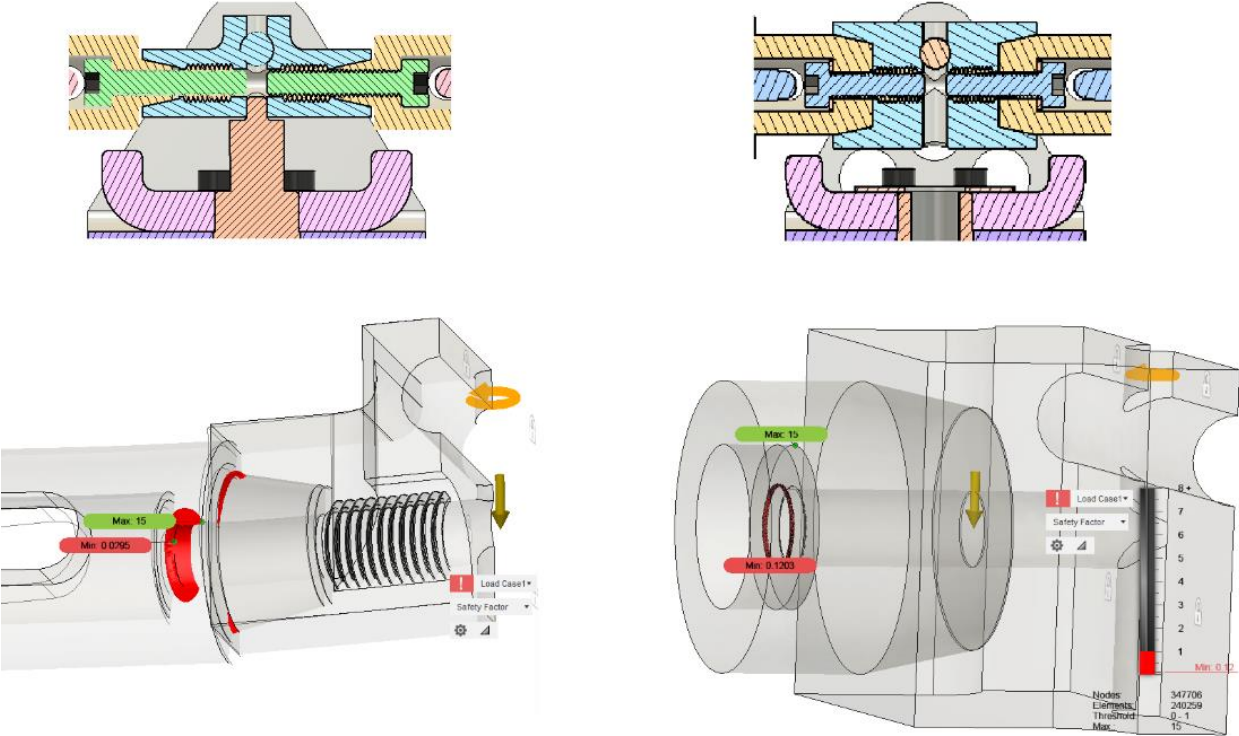


Figure 2.6. Initial and refined rotor head design. Left: tapered joint has too small dimensions, yielding in the tapered joint. Yielding will take place under the bolt head as well. Right: Improved design, yielding showing only under bolt head and much less of it.

After design improvements were made, a safety factor of 2 was reached in the tapered joint, but the simulation still showed yielding in aluminum under the bolt head. These results may be in part due to the sharp edge of the bolt hole in the simulation model which will not be the case in reality. Also, Machinery’s handbook suggests that this kind of bolt setup will not a problem. Furthermore, using higher preload will increase the fatigue life of the bolt considerably [32]. Since the main rotor blades would surely see cyclic load variations in the fully rigid state when flying with higher airspeeds, it was

decided against lowering the bolt preload. The high stresses in this area, in reality, will be dissipated and some yielding under the bolt head is acceptable. The contact true area increases and compressed material work hardens, being able to accept more load.

The third concern was finding out if the fixing pin would be able to reliably take the shear loads from asymmetric lift when the rotor is set up in a rigid configuration. FEA was run to investigate this as well and it was found that 4 mm diameter medium carbon steel pin would be able to take full asymmetric design loads - 1 blade creating full thrust and the other blade unloaded with a minimum safety factor of 1.6 before yielding (Fig. 2.7.). The hub was constrained in all axes but allowed to rotate around the teetering axis. Only simulation load applied was a remote force simulating blade lift acting at 274 mm from the rotation axis. Centrifugal forces were neglected because they will be cancelled out in the pin location due to symmetry. The fixing pin also serves a secondary purpose of centering the rotor head assembly on the main motor.

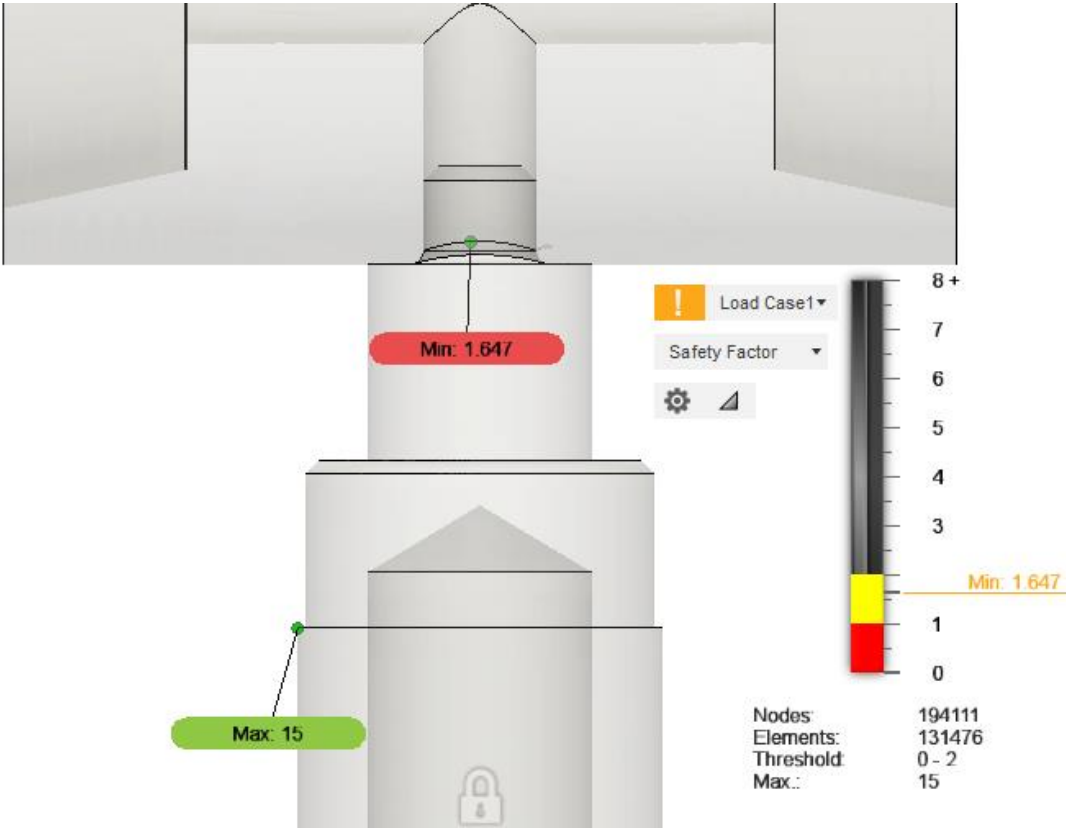


Figure 2.7. Fixing pin minimum safety factor at design load, fully asymmetric lift.

The vertical hole in the rotor hub where the fixing pin fits was designed as a through hole to also accommodate a balancing shaft. Careful balancing of the main rotor will be needed each time the

blades are removed, adjusted or if a second bolt is added to the blade holder to fix the lead-lag freedom.

The main rotor teetering needs to be limited by a mechanical stop that can absorb the residual energy and prevent the main rotor from contacting the booms rotors if the flight profile causes extreme teetering angles. A mechanical limiter was designed to absorb the energy from see-sawing and limit the maximum teetering angle to approximately  $7.5^\circ$  (Fig. 2.6. upper right section). The limiter will be 3D printed using polypropylene. PP was chosen because it has excellent toughness and relatively low modulus of elasticity – PP will absorb the energy more gradually than stiffer materials would and cause lower stresses to the rotor. Also, PP is readily available as FDM filament and 3D printing is the most flexible option for rapid prototyping.

A stainless-steel plate will be made to serve 2 purposes – act as a washer for the bolts attaching the teetering limiter to the rotor head bracket holding the teetering limiter more securely in place and to hold the fixing pin in position, if it is installed in the configuration which allows teetering (Fig. 2.2 middle).

## 2.6. Designing the housings for electronics

Electronics boards were divided vertically into 3 sections forming an electronics stack (Fig 2.8.). The best place for battery was found to be in the very bottom of the craft, so the power distribution boards form the first layer to keep power cables short. Middle layer is allocated to the ESC-s and top layer for the RC receiver, GPS receiver and the flight controller board. The first two floors also act as a structural member to stiffen the frame – the frame attaches to the lower two floors with 8 M3 bolts.

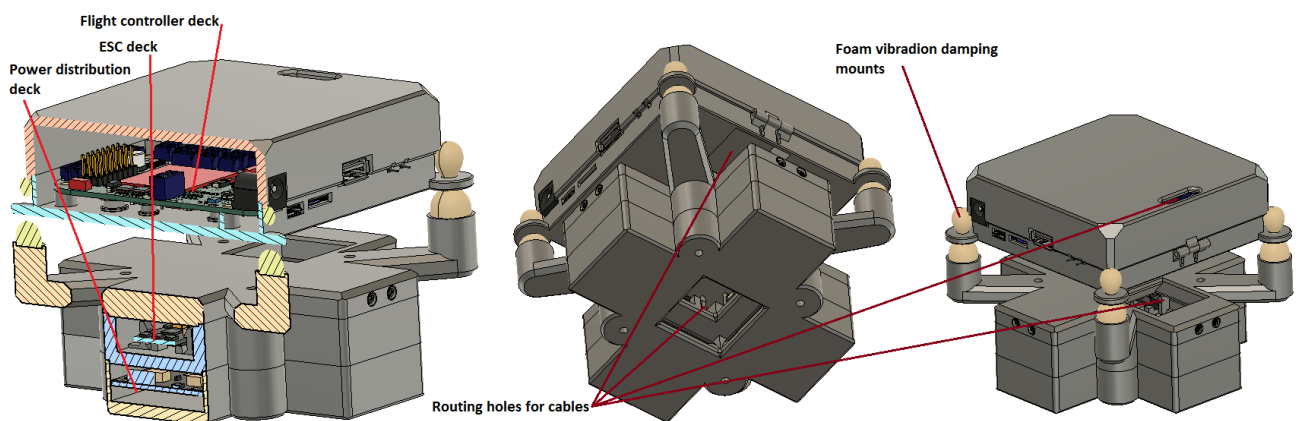


Figure 2.8. Electronics stack

The upper floor contains the flight controller board, which is also where the inertial measurement unit (IMU) is. This makes the flight control board quite sensitive to vibration, which is why the upper layer was designed to have a housing separated from the rest and to float on top of 4 vibration damping mounts. It was decided to use regular polyurethane foam ear plugs as vibration damping mounts because they are cheap, easy to acquire and they have been shown to be effective in damping vibrations in similar applications [33]. Also, they are very easy to mount – the bottom sides are glued to their mounting positions and upper sides are compressed to fit into the mounting holes of the flight controller housing. The ear plugs expand and form a good interference fit. It is also possible to tune the ear plugs to get the desired frequency response by controlling the height at which the flight controller housing attaches to the ear plugs. Ear plugs are available in a variety of shapes and softness, so there should be enough headroom for frequency tuning.

Ear plug mounting system was also experimentally tested by 3D printing PLA test bodies and joining them with an ear plug (Fig 2.9). This test was done to get quick qualitative results on how well does the interference fit hold, what is the best mounting hole diameter and how much abuse will the glued joint hold up. It was concluded that the best mounting hole diameter is 5mm and the interference fit and glued joint held up very well. Cyanoacrylate glue was used.



Figure 2.9. Testing the ear plug mounting method.

All housings for electronics were designed with cabling and avoiding electromagnetic interference in mind. Cables were designed to be run between the stack layers via central openings. Places to run the power cables though were designed to be as far from the flight controller as possible to limit possible electromagnetic interference (EMI) to the magnetometer and other low voltage electronics.

## 2.7. Designing the frame components

The frame was designed to be 3D printed and it consists of 2 parts. The lower part has mounting holes for the booms and it will house the battery and electronics (Fig. 2.11). The upper part attaches to the lower part with 8 M3 screws and it extends around the flight controller deck to allow the main motor to be mounted on top of it while still enabling access to the flight controller (Fig. 2.10). The frame was designed for 3D printing because rapid design iterations are possible with minimal effort of reaching a completed product from a CAD model. Furthermore, complex shapes are possible while keeping the cost for materials and machining low.



Figure 2.10. Upper Frame solid model and static stress simulation safety factor results.

The lower part of the frame was designed to house the Zippy Compact 6S 6200 mAh battery at the lower part of the frame because it is the largest single part of the drone and it would interfere with placement of other components if placed anywhere else (Fig. 2.11., 2.14). If it is mounted low in the frame, it will not get in the way of boom attachments and electronics keeping the vertical cross section low.

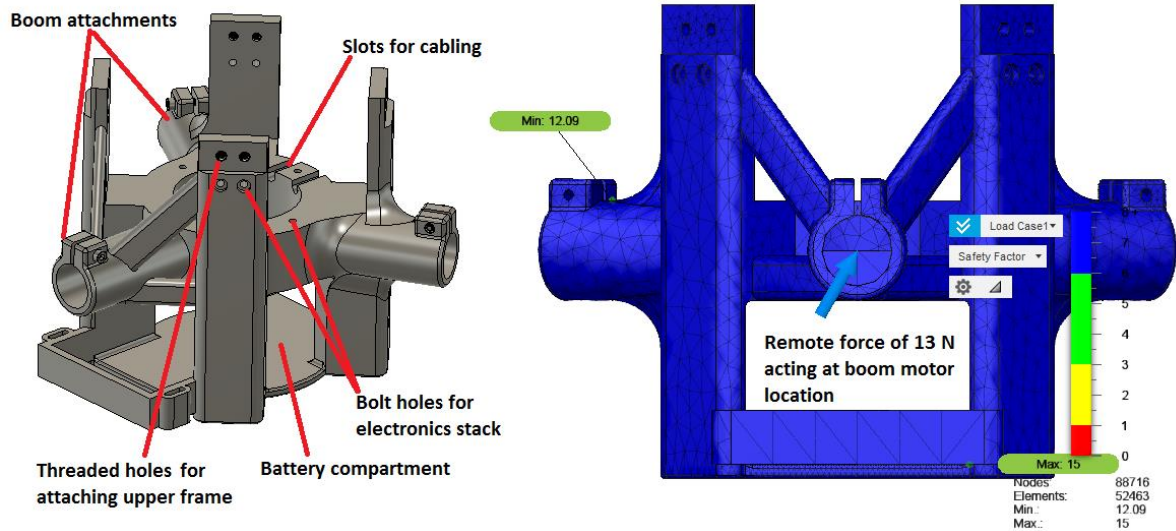


Figure 2.11. Lower frame and static stress analysis results. Minimum safety factor is 12.

Frame components were not weight optimized. Instead, they were designed with large strength excess due to uncertainties in the strength of 3D printed components loaded normal to print layers. Static stress simulations were run with FEA and minimum safety factor of 10 was achieved for both parts using the manufacturer's data on extruded material (Fig. 2.10., 2.11.). The parts were constrained in FEA with fixed constraints close to or at their intended attachment points and loaded with design loads. Material properties for PLA were defined according to manufacturer datasheet [28].

A 6063-T6 aluminum circular tube was selected to be used for the booms. A tube with 20 mm outer diameter and 1mm wall thickness is a standard dimension, so the material will be low cost and easy to acquire. Also, 6063-T6 aluminum tubing has good stiffness at reasonably low weight and more than enough strength for this application.

Mounts for attaching the boom motors to the boom were designed keeping possible vibration problems in mind. The boom motor mounting attachments and the boom attachments in the frame were designed with a large strength excess to keep the booms as rigid as possible. This will reduce the vibrations due to boom flex to a minimum and compensate for any inconsistencies in print quality. Slotted attachments are used for attaching both ends of the boom. An M3 bolt is used to reduce the diameter of the attachment and grip the boom firmly in place (Fig. 2.12.)



Figure 2.12. Boom motor mounts.  
CAD model and 3D printed test part with brass threaded insert.

The electronics stack (Fig 2.8.) will be bolted to the lower frame by 4 vertical and 8 horizontal bolts (Fig. 2.11). This ties all electronics housings and the frame into one solid piece further adding to the rigidity.

Landing gear will be made out of cut sections from a 110mm PP sewage pipe. Again, PP is an excellent material for landing gear, because it is very tough. The material is also readily available and cheap. Attachments were designed to attach the PP pipe sections to the booms (Fig. 2.13). These attachments will be 3D printed with PLA.



Figure 2.13. Landing gear PP-tube section and attachments

## 2.8. Mass, balance and performance

### 2.8.1. Masses

Masses of 3D printed components were estimated with the help of 3D slicing software IdeaMaker 3.3.0. Each mesh body was sliced with IdeaMaker which calculates the part mass based on filament length needed and density of the material used. This is a simple way of getting a result with reasonable accuracy for parts which do not use 100% infill. None of the 3D printed parts were sliced using an infill ratio of more than 30%, since usually the majority of strength and rigidity comes from the shell of the part being printed. Slicer settings in IdeaMaker were set as identical as possible to those used in RepetierHost. A boom motor mount was printed as a test and weighed on a scale with 0.1g resolution. The measured mass was 11.6g, the mass calculated by IdeaMaker was 12.2g, so a 5% difference exists. Since the difference between calculated and measured mass was low and the error was towards the safe side, it was deemed that the method is good enough to be used. Table 2.2 shows the estimated masses of all 3D printed components.

| Part                           | Material | No. of shells | Infill (%) | Estimated mass (g) |
|--------------------------------|----------|---------------|------------|--------------------|
| Upper frame                    | PLA      | 4             | 20         | 94.8               |
| Boom motor mount * 3           | PLA      | 4             | 20         | 12.2 * 3 = 36.6    |
| Lower frame                    | PLA      | 3             | 10         | 160.8              |
| Power distribution box         | PLA      | 2             | 10         | 32                 |
| ESC box                        | PLA      | 2             | 10         | 33.8               |
| ESC box cover                  | PLA      | 2             | 10         | 34.1               |
| Flight controller box          | PLA      | 2             | 10         | 28.2               |
| Flight controller box cover    | PLA      | 2             | 10         | 33.5               |
| Landing gear bracket upper * 3 | PLA      | 4             | 20         | 3.6 * 3 = 10.8     |
| Landing gear bracket lower * 3 | PLA      | 4             | 20         | 5.6 * 3 = 16.8     |
| Total mass of 3D printed parts | -        | -             | -          | <b>481.4</b>       |

Table 2.2. Estimated masses of 3D printed parts.

Mass of the rotor head assembly was estimated with the CAD software. A density of 2700 kg/m<sup>3</sup> was used for aluminum 6082 and built in values were used for steel. Mass estimation for the 3D printed PP teetering limiter was done the same way as described in previous section. The estimated masses of rotor head assembly components are listed in table 2.3.

| Part                            | Material                  | Estimated mass (g)  |
|---------------------------------|---------------------------|---------------------|
| Rotor hub                       | Aluminum 6082 T6          | 26 g                |
| Rotor hub threaded inserts (*2) | Stainless steel AISI 304  | $0.6 * 2 = 1.2$ g   |
| Blade holders (*2)              | Aluminum 6082 T6          | $11.5 * 2 = 23$ g   |
| Teetering bracket               | Aluminum 6082 T6          | 50g                 |
| Blade holder bolts M4x16 (*2)   | Steel ASTM F568M 12.9     | $2.3 * 2 = 4.6$ g   |
| Blade bolts M3x20 (*4)          | Steel ASTM F568M 8.8      | $1.4 * 4 = 5.6$ g   |
| Blade nuts M3 (*4)              | Steel and nylon           | $0.5 * 4 = 2$ g     |
| Teeter limiter                  | Polypropylene, 3D printed | 5.6 g               |
| Teeter limiter bolts M3x10 (*4) | Steel ASTM F568M 8.8      | $0.9 * 4 = 3.6$ g   |
| Teeter bearing spacer (*2)      | Aluminum 6082 T6          | $0.15g * 2 = 0.3$ g |
| Teeter bearing (*2)             | Steel                     | $1.5g * 2 = 3$ g    |
| Teeter shaft                    | Steel                     | 4.8 g               |
| Teeter shaft bolts M3x8 (*2)    | Steel ASTM F568M 8.8      | $0.8 * 2 = 1.6$ g   |
| Teeter bearing washer (*2)      | Steel                     | $0.15x2 = 0.3$ g    |
| Fixing pin                      | Steel                     | 18.9g               |
| Rotor head bolts M3x8 (*4)      | Steel ASTM F568M 8.8      | $0.8 * 4 = 3.2$ g   |
| Teeter limiter plate            | Stainless steel AISI 304  | 2.6g                |
| Rotor blades (*2)               | Carbon fiber composite    | $27.3 * 2 = 54.6$ g |
| Total mass of rotor head        | -                         | <b>210.9 g</b>      |

Table 2.3. Estimated mass of rotor head assembly

For initial calculations, the mass provided by manufacturers was used for all COTS hardware, except fasteners. Where reliable data was not available, a guess was made based on dimensions. The components were purchased and weighed using a scale with a 0.1 g resolution. The differences between estimated and measured values were small but they still existed. The masses of various COTS components are listed in table 2.4.

| Component                         | Mass estimated (g) | Mass measured (g)    |
|-----------------------------------|--------------------|----------------------|
| Flight controller                 | 36                 | 36                   |
| RC receiver                       | 4                  | 4,4                  |
| GPS receiver                      | 10                 | 7                    |
| Boom ESC (*3)                     | $7 * 3 = 21$       | $7.6 * 3 = 22,8$     |
| Power PDB (*4)                    | $7,3 * 4 = 29.2$   | $8 * 4 = 32$         |
| Main ESC                          | 14                 | 13,4                 |
| Main motor                        | 250                | 237.7                |
| Boom motors (*3)                  | $31.8 * 3 = 95.4$  | $36 * 3 = 108$       |
| Boom rotors (*3)                  | $4 * 3 = 12$       | $3.5 * 3 = 10.5$     |
| Battery                           | 835                | 843                  |
| Landing gear PP tube section (*3) | $12.7 * 3 = 38.1$  | 36.6                 |
| Aluminum booms (*3)               | $40.2 * 3 = 120.6$ | 120.6 (not measured) |
| Total                             | 1306.6             | <b>1472</b>          |

Table 2.4. Masses of COTS components

Other components not accounted for in previous tables are listed in table 2.5. The masses of various fasteners and other consumables like heat shrink tubing, glue, zip ties, cable connectors, solder *etc.* were only roughly estimated.

| Component(s)                                   | Estimated mass (g) |
|--|--------------------|
| Various fasteners not accounted for previously | 100                |
| Consumables                                    | 6                  |
| Cables   | 40                 |
| Total mass                                     | 146                |

Table 2.5. Masses of other components

These measured and estimated masses make the total mass of the craft to be 2310 g. Initial estimations using xCopterCalc showed the total mass range of the craft to be between 2 and 2.5 kg, which is in agreement with the results obtained by later estimations. The design goal of obtaining a total mass below 2.5 kg was reached.

**2.8.2. Balance**

The experimental Y4 was designed to be mostly symmetrical (Fig. 2.14). A major source of imbalance can be the battery due to its weight shifting around if not fixed correctly or if it is not mounted centrally. The lower part of the frame was designed to hold the center of mass of 6200 mAh Zippy Compact right under the main motor and it was designed specifically for this battery. This makes it practically impossible to mount the battery any other way than intended – with its center of mass under the rotational axis of the main motor.

The lower part of the frame is not ideally symmetrical due to it having a rectangular cross-section to accommodate the battery and electronics and at the same time have mounting attachments for 3 booms placed at equal angles from each other. Still, the frame is quite light and the mass offset it produces is quite low, so it is not expected that it will give a noticeable effect to the overall balance. If testing reveals that it does, there is room for some ballast masses to be added.



Figure 2.14. Experimental Y4 prototype – full CAD assembly

### 2.8.3. Performance

The maximum thrust from the main rotor ( $T_{mm}$ ) is expected to be 2957 g of force or  $T_{mm} = 29$  N with 28-inch propellers as stated by the manufacturer [20]. For the boom motors, the manufacturer states a maximum thrust of 18N with 5.1-inch 3-bladed propellers with 5-inch pitch. Since precise data is not available for the specific motor and propeller configuration, a conservative 15N is expected from chosen motor and propeller combination.

The maximum thrust that boom motors can provide to aid in lifting the craft depends on their cant angle, the length of the booms and the torque generated by the main rotor. Since the optimal cant angle will be determined experimentally,  $30^\circ$  as proposed by Driessens and Pounds [1] is used for calculations. The maximum thrust available in controlled hover depends on the torque produced by the main rotor, which needs to be balanced out. Any more thrust from the boom rotors would spin the craft around the vertical axis. The maximum torque produced by the main rotor ( $Q_m$ ) was estimated with eCalc design tool PropCalc to be  $\approx 1.8$  Nm. Since the boom motors were initially designed to be located ( $D_B$ ) 0.326 m from the vertical axis, this figure will be used as the moment arm for calculation. The horizontal thrust component from the boom motors needed to balance the main rotor torque is

$$T_h = Q_m/D_B, \quad (2.6)$$

where  $T_h$  – Combined horizontal thrust component of boom motors, N,

$Q_m$  – Main rotor torque, N\*m,

$D_b$  – Moment arm length from vertical axis to boom motor axis, m.

From equation 2.6 we see that  $T_h = 1.8 \text{ N*m} / 0.326 \text{ m} = \underline{5.5 \text{ N}}$ .

Since the boom motor cant angle of  $30^\circ$  is used for this calculation, a total thrust ( $T_t$ ) of

$T_t = T_h / \sin(30^\circ) = 5.5 \text{ N} / 0.5 = \underline{11 \text{ N}}$  is needed from the rotors. This gives a vertical thrust component

( $T_v$ ) of  $T_v = T_t * \cos(30^\circ) = 11 \text{ N} * 0.866 = \underline{9.5 \text{ N}}$ . This also means that each boom motor will contribute

with 1/3 of 11 N total thrust and 1/3 of 9.5 N of vertical thrust component at maximum balanced thrust

setting. This makes the boom motors quite overpowered and under-utilized for the application at  $30^\circ$

cant angle and leaves plenty of head room for further tweaking. It is expected that longer booms

necessitate lower cant angles and give better efficiency and higher maximum thrust at the cost of

increased weight of the booms and larger footprint.

The estimated all up mass of the prototype is 2310 g which gives a weight of 22.65 N. The maximum

thrust of the craft ( $T_{MAX}$ ) with 326 mm booms and a  $30^\circ$  cant angle for the boom motors is

$T_{MAX} = T_{mm} + T_v = 29 \text{ N} + 9.5 \text{ N} = \underline{38.5 \text{ N}}$ . This makes the initial thrust to weight ratio to be  $38.5/22.65 =$

1.7 with room for improvement when better optimized main rotor blades are used or the boom length

and cant angle are changed. The low thrust to weight ratio is mainly due to components not being

weight optimized and the use of a large battery. This thrust to weight ratio still allows full

maneuverability, albeit with higher demands on the main motor than ideal.

The estimated total current consumption of motors of the Y4 prototype in hover with a mass of 2310

g is ca 13 A according to xCopterCalc of eCalc. With the flight computer and other accessories

estimated to consume a conservative 3 A, the total current draw will be ca 16 A. LiPo batteries can be

safely discharged down to approximately 20% of their rated capacity. This means that a 6-cell 6200

mAh battery can be operated for approximately  $(6.2 \text{ Ah} * 0.8)/16 \text{ A} = 0.31$  hours or 19 minutes.

#### **2.8.4. Costs**

The cost of COTS components was logged in an Excel table. Shipping fees were included and the total

for any specific component was rounded to nearest integer. The costs of 3D printed components were

calculated considering the estimated mass of components, the price of unit mass of filament, the

approximate electricity usage and the depreciation of printer. An additional 10% was added to the

needed filament amount to account for the support structures and brims. An approximate cost of 200

€ was estimated for the entire rotor head, which includes materials, machining and COTS components.

Total costs are shown in table 2.6 and the details cost percentage of overall cost is shown in figure

2.15. The total costs reached 941 €, which is below the set goal of 1000 €. RC transmitter was not

included in the calculations, since this is not integral to the design and can be any FrSky compatible device. Since only one rotor head is planned to be produced, its design does not need to be optimized for scaled manufacturing. The cost of the rotor head seen in table 2.6 is the likely upper bound and is expected to be somewhat lower in practice based on an initial quote.

It can be seen that the rather complicated design of the main rotor head and the large main motor make up the biggest proportion of the overall costs. The battery, flight controller and ESC-s also give a sizeable contribution. It is reasonable to assume, that if future testing reveals the most successful main rotor configuration and control strategy, then much simpler main rotor design can be used and flight controller and other electronics can be optimized for the control strategy further lowering the cost. Furthermore, the main motor chosen for this prototype is a clone of the T-motor U8, which is a fairly expensive “pancake” design. Depending on the application, if reducing the size of the drone by about 1/3 is an option, or mass optimization is done, then noticeable cost reduction can be accomplished by using a smaller lower torque main motor.

| Item                  | Price (€)  |
|-----------------------|------------|
| Main rotor head       | 200        |
| Main motor            | 165        |
| Flight controller     | 90         |
| Battery               | 89         |
| ESC-s                 | 82         |
| Boom motors           | 80         |
| 3D printed components | 54         |
| GPS receiver          | 51         |
| Power distribution    | 40         |
| Main rotor blades     | 24         |
| Fasteners             | 40         |
| RC receiver           | 14         |
| Boom propellers       | 12         |
| <b>Total cost</b>     | <b>941</b> |

Table 2.6. Costs of Y4 prototype components

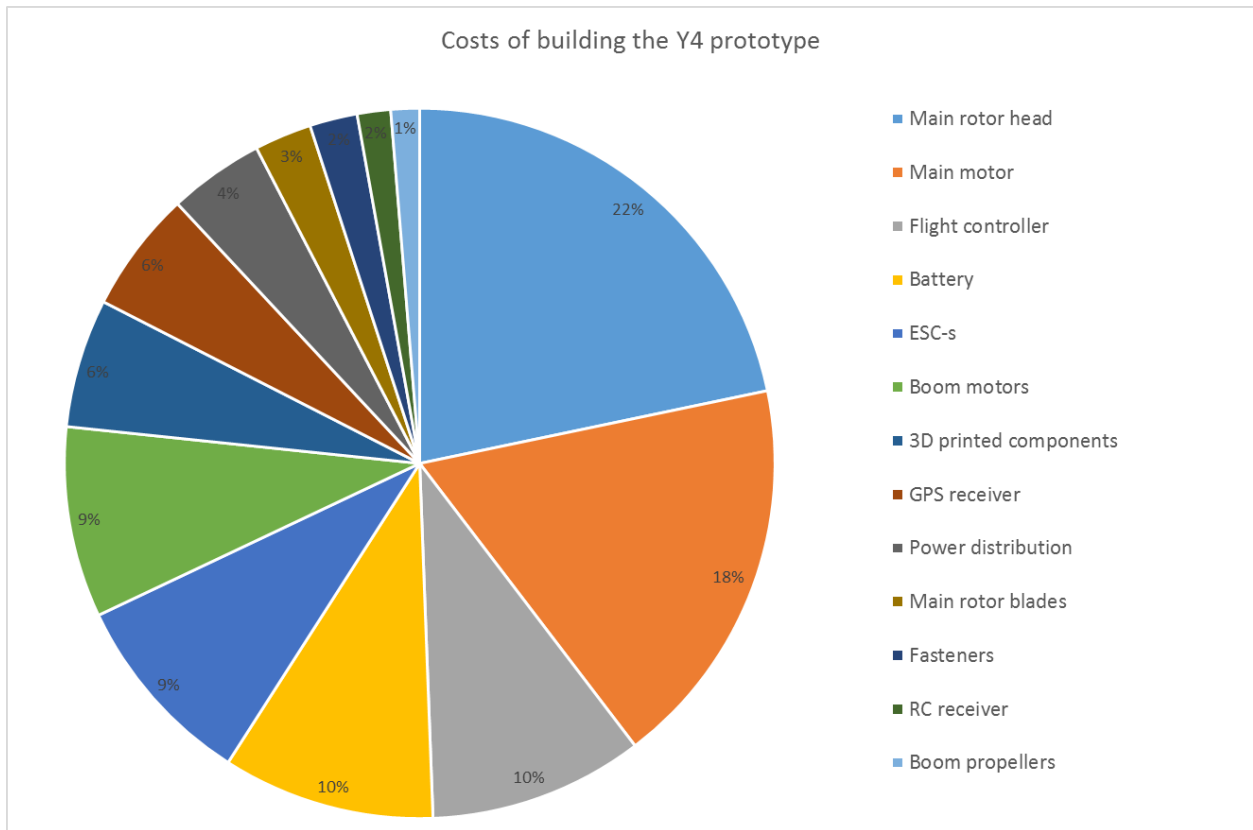


Figure 2.15. Percentages of overall cost

## 2.9. Future directions and applications

Finishing the build was not in the scope of this work, but it will be the next obvious step towards reaching the long-term goals of this investigation. 3D printed components will be printed in the first order and their strength tested non-destructively with twice the design load. It is also possible, that a further weight reduction can be achieved in the future by optimizing the shell count and infill density of 3D printed components. To achieve this, test bodies need to be printed and tested. If it becomes apparent that the strength of the 3D printed components is unnecessarily high and further weight reduction is needed, new components can be printed.

Rotor head components also need to be machined and various fasteners acquired. Main rotor assembly needs to be carefully balanced prior to mounting on the motor. Balancing is planned to be done using a standard RC rotor balancing stand with a 3 mm balancing shaft. The rotor hub and blade holder assembly will be balanced first, then the blades will be attached and balancing will be done again. This way the rotor head and blades will be balanced independently of each other, but also as an

assembly. For balancing the hub and blade holders, material removal will be used. For the blades, weight will be added to achieve balance.

When the prototype is assembled, control software needs to be written and vibration damping tuned. For this purpose, initially it is planned to modify existing open source software – ArduCopter and dampen the vibrations to as low as practically reasonable. Later, it is planned to experiment with hybrid control strategies on rigid and teetering setup that have better predictive capabilities than PID.

To safely test and tune stability and control, building a test stand would be preferable. This way, the risk of damaging the craft during initial testing is reduced significantly. There are several options for the construction of this stand with various difficulty levels and degrees of freedom they allow. A stand that would allow all 6 degrees of freedom while restraining the craft within safe limits would be preferable. Possible alternatives with their flaws are depicted on figure 2.16 and figure 2.17.

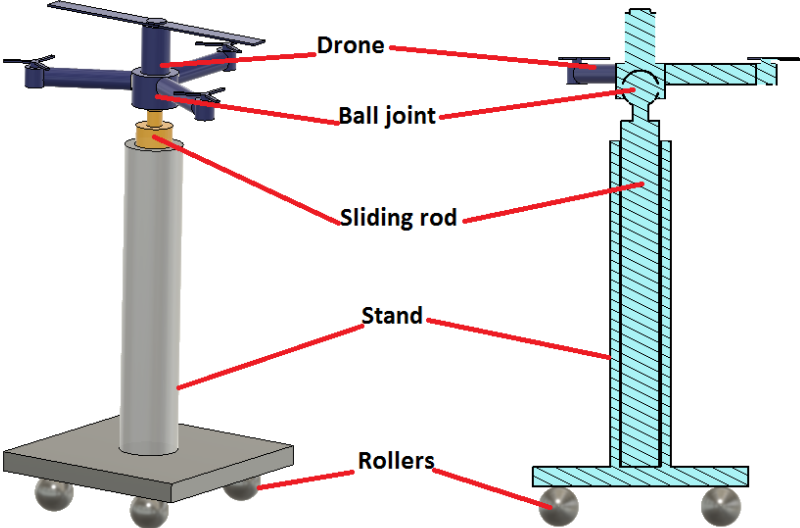


Figure 2.16. Possible test stand no. 1. Roll, pitch and yaw are accommodated by ball joint, horizontal translations by rollers and vertical translation by sliding rod. With this design, the mass of the stand would affect the dynamics of the drone. Refined idea from source [42].

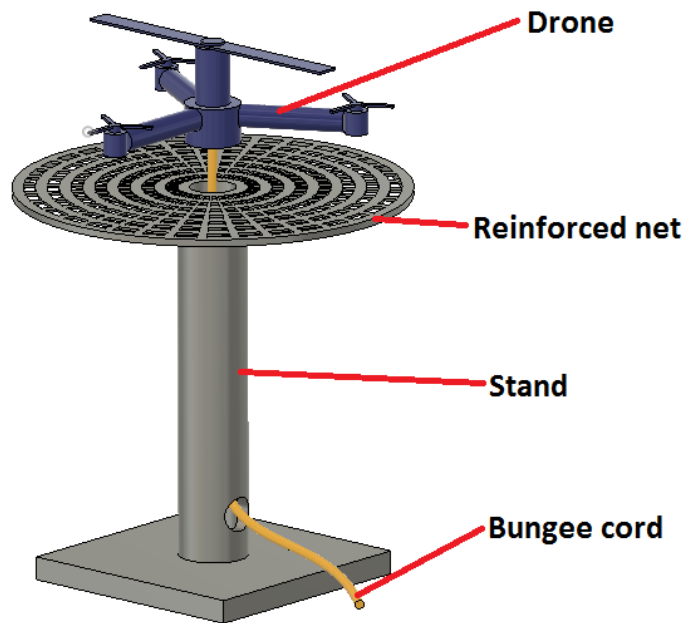


Figure 2.17. Possible test stand no. 2.

All 6 degrees of freedom are allowed. Drone is restrained by bungee cord which can be used to pull the craft against reinforced net platform if needed. The cord does not affect the dynamics much, but accurate restraint and crash avoidance is not guaranteed. Source: [43]

If an adequate control strategy has been implemented and stable flight achieved, different boom lengths, boom motor cant angles and upper frame heights can be tested to find the optimum. As Driessens and Pounds suggested, placing the boom rotors outside the *vena contracta* could give added stability and efficiency [1]. It has been shown that the wake of an isolated rotor will contract down to 75% of the rotor diameter at 0.35 diameter distance downstream from the rotor plane [21], so reduced flow velocity and disturbances outside this area might give desirable results.

Next, high speed tests can be conducted to establish the full flight envelope of the craft and establish its ability to fight the dissymmetry of lift. If the dissymmetry becomes a major problem for stability or efficiency, possible countermeasures can be explored. Possible alternatives would be maintaining the teetering hinge or augmenting the lift using fixed lifting surfaces. Both options would add complexity to the design, but would still be simpler than traditional helicopter or hybrid VTOL aircraft control systems. Then, using the knowledge gained, an optimized prototype can be built for a specific purpose.

Since, beyond doubt, fixed wing and hybrid VTOL platforms are a better option for long distance and endurance operations, Y4 platform would be better suited for short distance missions, where robust VTOL capability is needed and landing space is at premium. Thanks to its small footprint and good efficiency, Y4 could be best suited for short distance parcel delivery in urban or suburban

environments, power-tethered applications and aerial photography, small-scale aerial surveillance or inspections. Unfortunately, due to scaling laws, all platforms relying on rapidly changing the angular velocity of rotors make more sense when they are small [\[36\]](#).

## Summary

Battery powered drones are bound to become more and more prevalent in applications where the offset or reduced pollution, minimized noise and potential for global environmental sustainability outweigh the low energy density of batteries. When comparing different platforms, fixed wing aircraft are far more efficient than rotary wing solutions, but the robust VTOL capability of multicopters and helicopters still necessitates their use in areas with difficult terrain. Thus, battery powered multirotor drones will likely see increased use in short range and complicated terrain scenarios. Therefore, in light of ever-increasing commercial use of these drones, raising their aerodynamic efficiency needs to be addressed. Lowering the disc loading of rotors to combat induced losses is one possible direction to accomplish this.

In this thesis, an unconventional quadrotor prototype was designed based on the Y4 triquad configuration proposed by Driessens and Pounds in 2013. The prototype was devised to address the unanswered questions and solve the problems currently inhibiting the commercial adoption of Y4-type drones. Y4 promises helicopter-like efficiency combined with quadcopter-like simplicity and robustness. Y4 has one large central rotor which provides the majority of lift and keeps the disc loading low. Additionally, it has 3 smaller propellers mounted at an angle from the horizontal at the ends of 3 booms extending from the fuselage to provide counter-torque and control. All rotors are fixed pitch propellers, so the only control method is changing the speed of the motors making the drone quite simple and robust. The Y4 prototype designed in this thesis was devised with a highly configurable main rotor to enable further research into solving the problems with the original configuration and step towards realizing the large aerodynamic efficiency gains promised while maintaining the simplicity.

Initially, back-of-the-envelope calculations were done and COTS hardware was selected. Based on the main motor and rotor combination chosen, a rotor head that can allow switching between fully rigid or teetering operation was designed. In addition, blade pitch can easily be adjusted and lead-lag freedom allowed or restricted. Moreover, the main rotor head can accommodate rotor blade upgrades with blades twice as massive as used in the initial design. The frame, various attachments and electronics housings for the drone were designed to be 3D printed. To verify the strength of critical components, FEA simulations were done. The results show that the prototype would weigh 2310 g, have thrust-to-weight ratio of 1.7 and can hover up to 19 minutes with the selected battery. Estimated cost of building the prototype is 941€. All things considered, the design targets set on mass, cost and performance were met.

The motivation for designing a new Y4 prototype was to obtain an experimental platform where the dynamics of fully rigid setup can be thoroughly investigated and directly compared to the teetered head version. The described prototype developed in this thesis allows this comparison to be easily done while maintaining identical hardware. In future development, hybrid control strategies can be tested to enable reaching a stable and highly efficient machine.

## Kokkuvõte

Akutoitega droonid leiavad üha enam kasutust rakendustes, kus geograafiliselt hajutatud või vähendatud reostamine, müra vähendamine ja globaalse keskkonnahoiu potentsiaal kaaluvad üles akude madala energiatiheduse. Erinevaid platvorme võrreldes on lennukid palju efektiivsemad kui kopterid, kuid multikopterite ja helikopterite robustne VTOL-võimekus tingib endiselt nende kasutamist keerulise maastikuga piirkondades. Akutoitega multikopterite kasutamine laieneb lähitulevikus tõenäoliselt märkimisväärselt just lühimaa lendudel ja keerulise maastikuga stsenaariumides. Selliste lennuvahendite üha laieneva kasutamise valguses tuleb seetõttu tegeleda nende aerodünaamilise efektiivsuse parendamisega. Rotoriketta pindalaühikule langeva koormuse vähendamine indutseeritud kadude vastu võitlemiseks on üks võimalik suund selle saavutamiseks.

Käesolevas töös projekteeriti ebahariliku ehitusega neljarootorilise drooni prototüüp, mis põhineb Driessens'i ja Pounds'i poolt 2013. aastal välja pakutud Y4 kolmikkonfiguratsioonil. Käesolevas töös käsitletud prototüüp töötati välja võimaldamaks probleemide lahendamist, mis on siiani Y4-tüüpi droonide kaubanduslikku levikut takistanud. Y4 lubab helikopterilaadset efektiivsust multikopteritele omase lihtsuse ja vastupidavusega. Y4 kasutab ühte kesket suurt rootorit, mis annab enamiku tõstejõust tagades madala koormuse rootoriketta pindalaühiku kohta. Lisaks on sellel 3 väiksemat propellerit, mis on paigaldatud nurga all horisontaaltasapinna suhtes kolme raami õla otstes, et tagada vastuväändemoment pearootorile ja drooni juhtimine. Kõik rootorid on fikseeritud sammuga propellerid, seega ainus asendi kontrolli meetod on mootorite kiiruse muutmine. See teeb Y4 sama lihtsaks ja robustseks nagu harilikud multikopterid. Käesolevas töös kavandatud Y4 prototüüp töötati välja mitmeti seadistatava pearootoriga, et võimaldada täiendavaid uuringuid Driessens'i ja Pounds'i poolt välja pakutud konfiguratsiooni probleemide lahendamiseks. See võimaldab astuda sammu lähemale suurema aerodünaamilise efektiivsuse realiseerimisele, samas säilitades ehituse lihtsuse.

Esiialgu tehti ligikaudsed arvutused ja valiti kaubanduses saadaolev riistvara. Valitud peamootori ja pearootori kombinatsiooni põhjal konstrueeriti rootoripea, mis võimaldab valida täielikult jäiga või kiige liigendiga seadistuse vahel. Lisaks on kergelt reguleeritav rootorilabade seadenurk ning rootoritasapinnas saab labade liikumisvabadust normaalasukohast ette või tahapoole lubada või piirata. Peale selle on rootoripea piisava tugevusega, et tulevikus võib pearootorit uuendada labadega, mis on kuni kaks korda suurema massiga kui käesolevas töös kirjeldatud labad. Raamikomponendid, erinevad kinnitused ja elektroonika korpused projekteeriti 3D-prinditavatena. Kriitiliste komponentide tugevuse kontrollimiseks viidi läbi FEA simulatsioonid. Töö tulemused näitavad, et prototüüp kaaluks 2310 g, tõstejõu ja kaalu suhe on 1,7 ja valitud akuga saab kuni 19 minutit ripplennus lennata. Prototüübi ehitamise hinnanguline maksumus on 941 eurot. Kõiki kaalutlusi silmas pidades, said massi, maksumuse ja jõudluse jaoks seatud eesmärgid täidetud.

Uue Y4 prototüübi projekteerimise mõte oli saada eksperimentaalne platvorm, kus täielikult jäiga rootoriseadistuse dünaamikat saab põhjalikult uurida ja otseselt võrrelda kiigeliigendiga rootoriga. Käesolevas töös välja töötatud prototüüp võimaldab seda võrdlust hõlpsasti teha samal riistvaral. Tulevikus testitakse prototüübil hübriidkontrollistrateegiaid ning töötatakse välja toimiv lahendus, et saavutada stabiilne ja kõrge efektiivsusega multikopter.

## References

1. Driessens, S., Pounds, P. Towards A More Efficient Quadrotor Configuration. Conference Paper in Proceedings of the IEEE/RSJ International Conference on Intelligent Robots and Systems. IEEE/RSJ International Conference on Intelligent Robots and Systems. 2013.
2. Craig, G. M. Physical principles of winged flight. 2009. <http://regenpress.com/aerodynamics.pdf> (25.05.2019)
3. AAIB Bulletin No: 5/2005. Excerpt from AAIB Field Investigation. R44 crash investigation report. [https://assets.publishing.service.gov.uk/media/54230420ed915d1371000c93/G-OUEL\\_5-05.pdf](https://assets.publishing.service.gov.uk/media/54230420ed915d1371000c93/G-OUEL_5-05.pdf) (25.05.2019)
4. Motor constants. Wikipedia, The free encyclopedia [https://en.wikipedia.org/wiki/Motor\\_constants](https://en.wikipedia.org/wiki/Motor_constants) (25.05.2019)
5. DShot and BLHeli ESC Support. Ardupilot Copter documentation. <http://ardupilot.org/copter/docs/common-dshot.html> (25.05.2019)
6. Beaglebone Blue. Website. <https://beagleboard.org/blue> (25.05.2019)
7. ROS: The Linux for Robotics. Nootrix website. <https://nootrix.com/diy-tutos/ros/> (25.05.2019)
8. Plessis, J., Pounds, P. Rotor Flapping for a Triangular Quadrotor. Conference paper in Australasian Conference on Robotics and Automation. 2014.
9. BeagleBone Blue Robotics Controller Kit - Linux – Review. 2017. <https://www.element14.com/community/roadTestReviews/2517/l/beaglebone-blue-robotics-controller-kit-linux-review> (25.05.2019)
10. Strawson, J. Robot Control Library. Servo. [http://strawsondesign.com/docs/librobotcontrol/group\\_servo.html](http://strawsondesign.com/docs/librobotcontrol/group_servo.html) (25.05.2019)
11. McLean, D. Wingtip Devices: What They Do and How They Do It. Boeing – Aerodynamics. Performance and Flight Operations Engineering Conference. 2005.
12. Nootebos, S. Aerodynamic Analysis and Optimisation of Wingtip-Mounted Pusher Propellers. An investigation into the propulsive gains and optimal geometry of small-scale propellers. MSc. Thesis TU Telft. 2018. <https://repository.tudelft.nl/islandora/object/uuid:83c88c41-3fa0-4ddb-9cc2-b5e574d0cd6a/datastream/OBJ/download>
13. Van Hare, T. C. Flight stories. De la Cierva. Historic Wings online magazine. 2013. <http://fly.historicwings.com/2013/06/de-la-cierva/> (25.05.2019)
14. Cantrell, P. Helicopter Aerodynamics. <http://www.mionome.com/Uni/Helicopter%20Aerodynamic.pdf> (25.05.2019)

15. Maisel, M. D., Giulianetti, D. J., Dugan, D. C. The History of the XV-15 Tilt Rotor Research Aircraft: From Concept to Flight. Monographs in Aerospace History #17. 2000. <https://history.nasa.gov/monograph17.pdf> (25.05.2019)
16. T-motor e-store. G28×9.2 Prop-2PCS/PAIR. <http://store-en.tmotor.com/goods.php?id=409> (25.05.2019)
17. FAA helicopter flying handbook. Chapter 4. Helicopter components, sections and systems. [https://www.faa.gov/regulations\\_policies/handbooks\\_manuals/aviation/helicopter\\_flying\\_handbook/media/hfh\\_ch04.pdf](https://www.faa.gov/regulations_policies/handbooks_manuals/aviation/helicopter_flying_handbook/media/hfh_ch04.pdf) (25.05.2019)
18. Metric bolts, screws & nuts tightening torques. Fastener Mart. [https://www.fastenermart.com/files/metric\\_tighten\\_torques.pdf](https://www.fastenermart.com/files/metric_tighten_torques.pdf) (25.05.2019)
19. Minimum ultimate tensile and proof loads for metric bolts with coarse or fine threads. [https://www.engineeringtoolbox.com/metric-bolts-minimum-ultimate-tensile-proof-loads-d\\_2026.html](https://www.engineeringtoolbox.com/metric-bolts-minimum-ultimate-tensile-proof-loads-d_2026.html) (25.05.2019)
20. Maytech 8626 130KV remote control electric motor U8 size for UAV with 40% off (1pcs). <https://www.aliexpress.com/item/Maytech-8626-130KV-remote-control-electric-motor-U8-size-for-UAV-with-40-off-1pcs/32694753204.html> (25.05.2019)
21. Taylor, M., K. A Balsa-dust technique for air-flow visualization and its application to flow through model helicopter rotors in static thrust. National Advisory Committee for Aeronautics. 1950. <https://ntrs.nasa.gov/archive/nasa/casi.ntrs.nasa.gov/19930082865.pdf> (01.05.2019)
22. Friction theory and coefficients of friction for ice, aluminum, steel, graphite and other common materials and materials combinations. [https://www.engineeringtoolbox.com/friction-coefficients-d\\_778.html](https://www.engineeringtoolbox.com/friction-coefficients-d_778.html) (25.05.2019)
23. SparkFun GPS Breakout - XA1110 (Qwiic) Hookup Guide. <https://learn.sparkfun.com/tutorials/sparkfun-gps-breakout---xa1110-qwiic-hookup-guide?> (25.05.2019)
24. XSR. FrSky 2.4 GHz receiver. <https://www.frsky-rc.com/product/xsr/> (25.05.2019)
25. BeagleBone Blue. [https://docs.px4.io/en/flight\\_controller/beaglebone\\_blue.html](https://docs.px4.io/en/flight_controller/beaglebone_blue.html) (25.05.2019)
26. Hobbywing XRotor Race Pro 2207 1750Kv Motor – Black. <https://www.getfpv.com/hobbywing-xrotor-race-pro-2207-1750kv-motor-black.html> (25.05.2019)
27. Constraints. Autodesk Fusion 360 documentation. <http://help.autodesk.com/view/fusion360/ENU/?guid=GUID-CBF8B62A-2498-462E-97E8-604D570EE022> (25.05.2019)
28. PLA and ABS Strength data. ASTM D256, D695, D638, D790. [http://download.makerbot.com/legal/MakerBot\\_R\\_PLA\\_and\\_ABS\\_Strength\\_Data.pdf](http://download.makerbot.com/legal/MakerBot_R_PLA_and_ABS_Strength_Data.pdf) (25.05.2019)

29. Everything you need to know about PLA. Rogers, T. Creative mechanisms blog. 2015. <https://www.creativemechanisms.com/blog/learn-about-poly-lactic-acid-pla-prototypes> (25.05.2019)
30. Everything you need to know about Polypropylene (PP). Creative mechanisms staff. Creative mechanisms blog. 2016. <https://www.creativemechanisms.com/blog/all-about-polypropylene-pp-plastic> (25.05.2019)
31. Steep Tapers & Fast Tapers. AT3 and What It Means. Benish, D. Blog post D&L Industrial INC. 2012. <http://www.dlindustrial.com/profiles/blogs/steep-tapers-fast-tapers-at3-and-what-it-means> (25.05.2019)
32. Oberg, E., Jones, F. D., Horton, H. L., Ryffel, H. H. Machinery's handbook. 26<sup>th</sup> edition. Industrial press. 2000.
33. Vibration damping – Copter documentation. <http://ardupilot.org/copter/docs/common-vibration-damping.html?highlight=vibration> (25.05.2019)
34. Pounds, P. Design, Construction and Control of a Large Quadrotor Micro Air Vehicle. Doctoral thesis, The Australian National University. 2007.
35. Chapman, A. Types of Drones: Multi-Rotor vs Fixed-Wing vs Single Rotor vs Hybrid VTOL. Australian UAV. <https://www.auav.com.au/articles/drone-types/> (25.05.2019)
36. Bangura, M., Melega, M., Naldi, R., Mahony, R. Aerodynamics of Rotor Blades for Quadrotors. Australian National University. 2016. <https://arxiv.org/pdf/1601.00733.pdf> (25.05.2019)
37. Ricardo, B. Using scaling to compute moments of inertia of symmetric objects. European Journal of Physics. 2015. [https://www.researchgate.net/publication/279071012\\_Using\\_scaling\\_to\\_compute\\_moments\\_of\\_inertia\\_of\\_symmetric\\_objects](https://www.researchgate.net/publication/279071012_Using_scaling_to_compute_moments_of_inertia_of_symmetric_objects) (25.05.2019)
38. Vandoren, V. To PID or not to PID. Control engineering. 2017. <https://www.controleng.com/articles/to-pid-or-not-to-pid/> (25.05.2019)
39. Li, L., Sun, L., Jin, J. Survey of Advances in Control algorithms of Quadrotor Unmanned Aerial Vehicle. Proceedings of ICCT 2015.
40. Giovanini, L. Predictive feedback control: an alternative to proportional–integral–derivative control. Journal of Systems and Control Engineering. Vol 223. 2009.
41. Stolaroff, J. K., Samaras, C., O'Neill, E. R., Lubers, A., Mitchell, A. S., Ceperley, D. Energy use and life cycle greenhouse gas emissions of drones for commercial package delivery. Nature Communications. 2018.
42. Barbosa, F. 4DOF quadcopter: Development, modelign and control. Masters thesis. Escola Politecnica of Universidade de Sao Paulo. 2017.

43. Giurdano, R. Test Stand Setup? DIY DRONES forum thread.  
<https://diydrones.com/forum/topics/test-stand-setup?groupUrl=arducopterusergroup&>  
(10.05.2019)
44. Sridharan, A., Govindarajan, B., Nagaraj, V. T., Chopra, I. Towards Coupling of Comprehensive Analysis into Design Sizing of a High-Speed Asymmetric Compound Helicopter. University of Maryland. 2017.
45. Osenar, P., Sisco, J., Reid, C. Advanced Propulsion for Small Unmanned Aerial Vehicles. The Role of Fuel Cell-Based Energy Systems for Commercial UAVs. Ballard, white paper. 2017.

## **Graphics**

**Y4 Drone assembly drawing 1:5; Sheet - A3**

**Main motor assembly drawing 1:4; Sheet – A3**

**Teetering bracket drawing 1:1; Sheet – A4**

**Rotor hub drawing 1:1; Sheet – A4**

**Blade holder drawing 1:1; Sheet – A4**

**Fixing pin drawing 2:1; Sheet – A4**

**Teetering shaft drawing 2:1; Sheet – A4**

**Teetering spacer drawing 5:1; Sheet – A4**

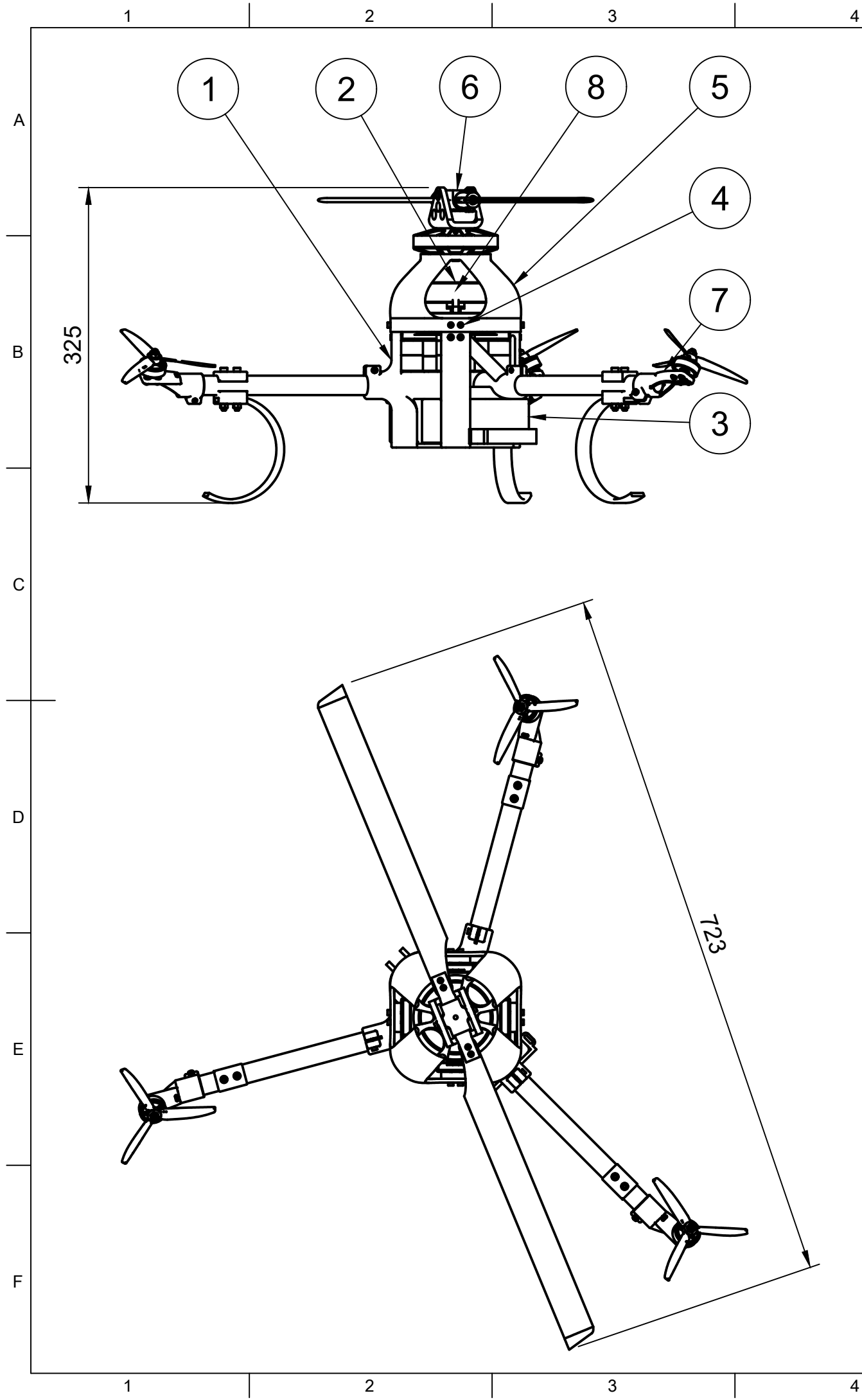
**Face plate drawing 2:1; Sheet – A4**

**Boom motor assembly drawing 1:4; Sheet – A4**

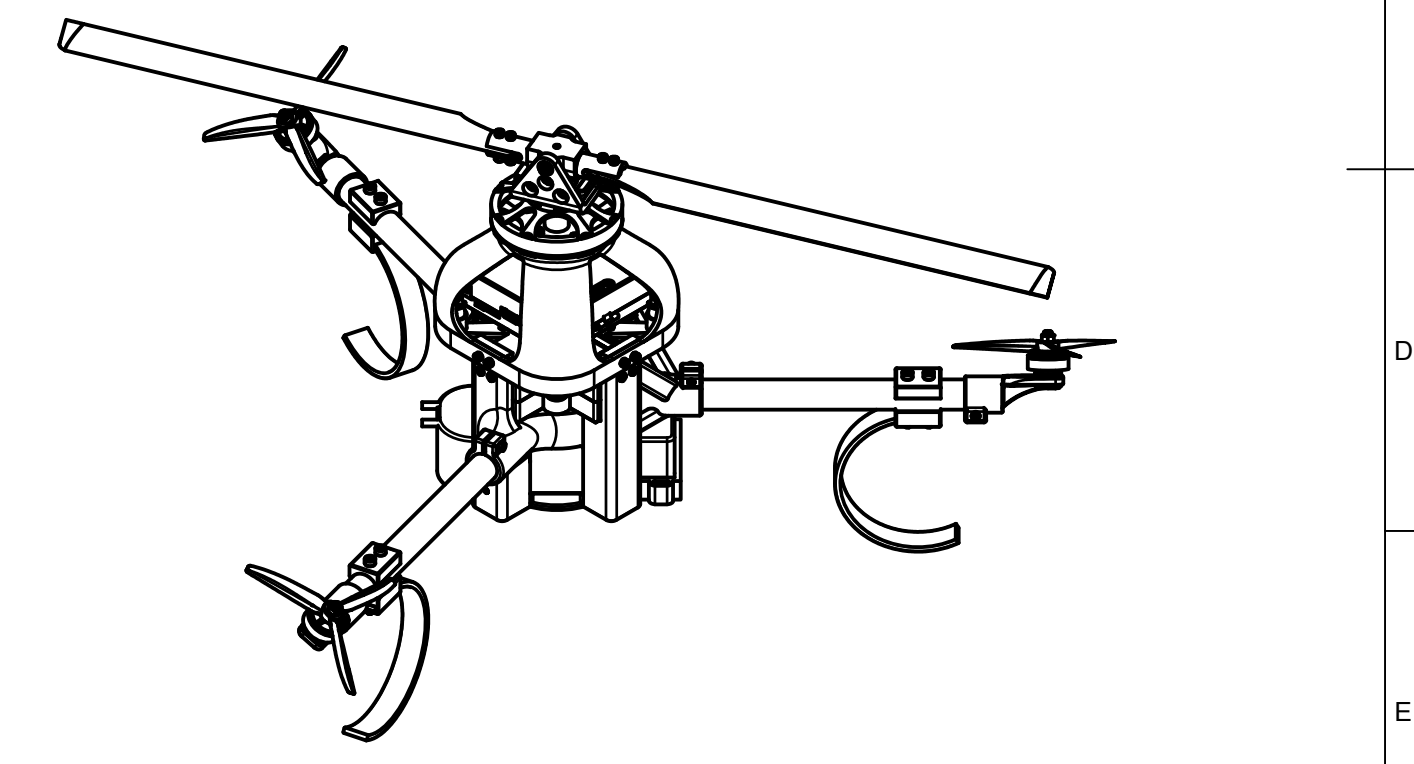
**Boom drawing 1:2; Sheet – A4**

**Polypropylene 110mm pipe section drawing 1:2; Sheet – A4**

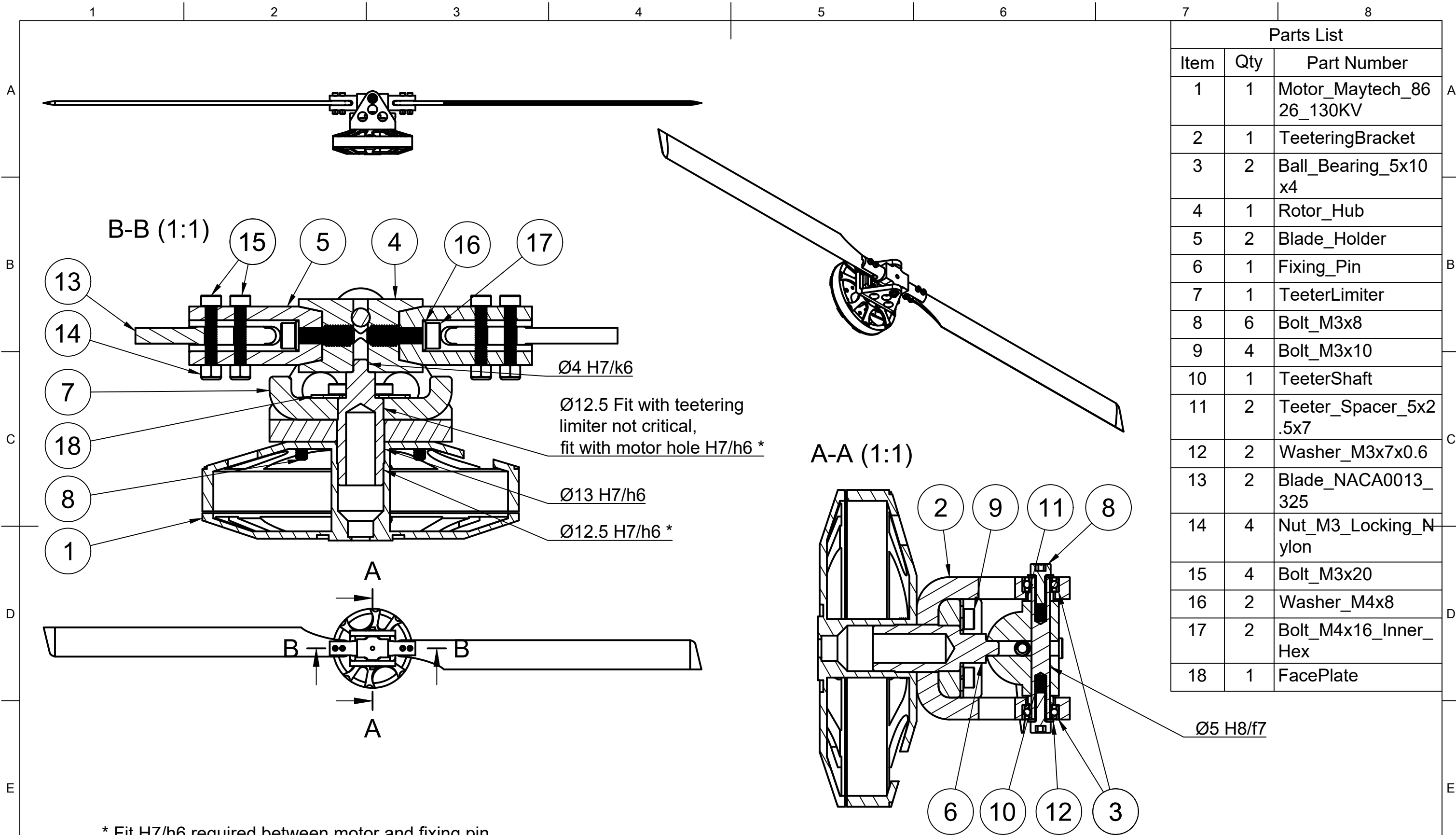
**Electronics stack assembly 1:2; Sheet – A3**



| Parts List |     |                                 |             |          |
|------------|-----|---------------------------------|-------------|----------|
| Item       | Qty | Part Number                     | Description | Material |
| 1          | 1   | Frame_Lower                     |             |          |
| 2          | 1   | ElectronicsStackAs sy           |             |          |
| 3          | 1   | Battery_Zippy_Co mpact_6200_40C |             |          |
| 4          | 16  | Bolt_M3x12                      |             | Steel    |
| 5          | 1   | Frame_Upper                     |             | PLA_3D   |
| 6          | 1   | MainMotorAssy                   |             |          |
| 7          | 3   | BoomMotorAssy                   |             |          |
| 8          | 4   | Bolt_M4x10                      |             | Steel    |



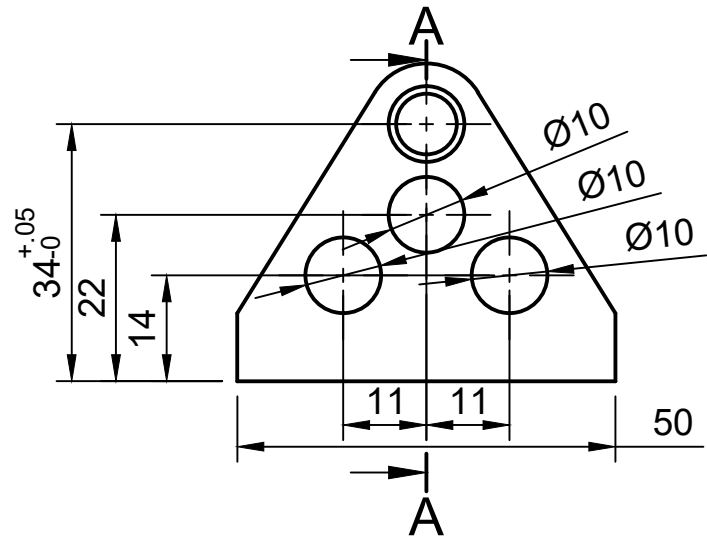
|       |                     |  |                 |             |
|-------|---------------------|--|-----------------|-------------|
| Dept. | Technical reference | Created by<br><b>Ott Tahk</b>                    | 18.05.2019      | Approved by |
|       |                     | Document type                                    | Document status |             |
|       |                     | Title<br><b>R_01_00_00<br/>Y4 drone assembly</b> | DWG No.         |             |
| Rev.  | Date of issue       | Sheet  |                 | 1/1         |



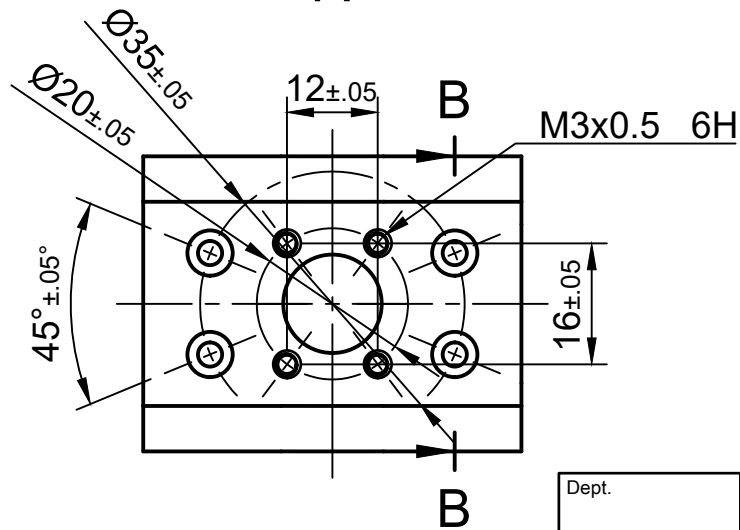
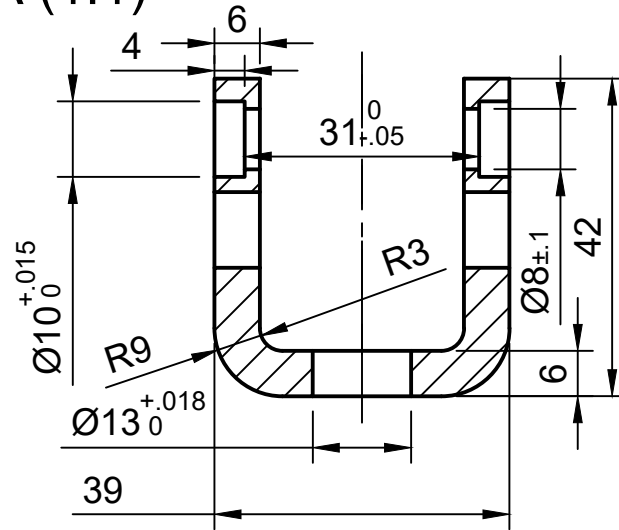
| Parts List |     |                              |
|------------|-----|------------------------------|
| Item       | Qty | Part Number                  |
| 1          | 1   | Motor_Maytech_86<br>26_130KV |
| 2          | 1   | TeeteringBracket             |
| 3          | 2   | Ball_Bearing_5x10<br>x4      |
| 4          | 1   | Rotor_Hub                    |
| 5          | 2   | Blade_Holder                 |
| 6          | 1   | Fixing_Pin                   |
| 7          | 1   | TeeterLimiter                |
| 8          | 6   | Bolt_M3x8                    |
| 9          | 4   | Bolt_M3x10                   |
| 10         | 1   | TeeterShaft                  |
| 11         | 2   | Teeter_Spacer_5x2<br>.5x7    |
| 12         | 2   | Washer_M3x7x0.6              |
| 13         | 2   | Blade_NACA0013_325           |
| 14         | 4   | Nut_M3_Locking_Nylon         |
| 15         | 4   | Bolt_M3x20                   |
| 16         | 2   | Washer_M4x8                  |
| 17         | 2   | Bolt_M4x16_Inner_Hex         |
| 18         | 1   | FacePlate                    |

\* Fit H7/h6 required between motor and fixing pin  
Fixing pin should have the same fit with motor if installed upside down

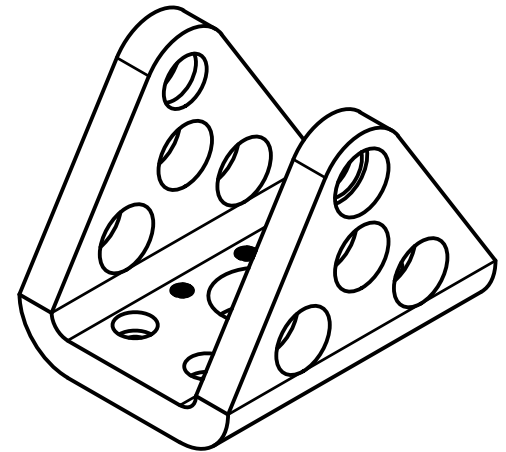
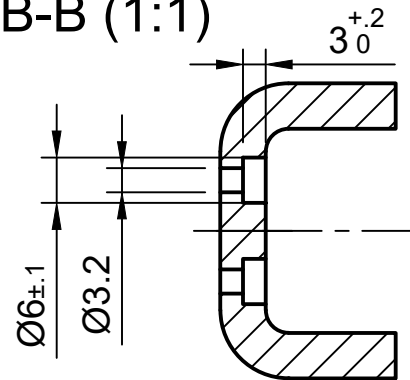
|   |                     |                               |                 |             |
|---|---------------------|-------------------------------|-----------------|-------------|
| Dept.   | Technical reference | Created by<br><b>Ott Tahk</b> | 20.05.2019      | Approved by |
| <br><b>TTU</b><br>DEPARTMENT OF MECHANICAL<br>AND INDUSTRIAL ENGINEERING |                     | Document type                 | Document status |             |
|   |                     | Title<br><b>MainMotorAssy</b> | DWG No.         |             |
| Rev.  | Date of issue       | Sheet<br><b>1/1</b>           |                 |             |



A-A (1:1)

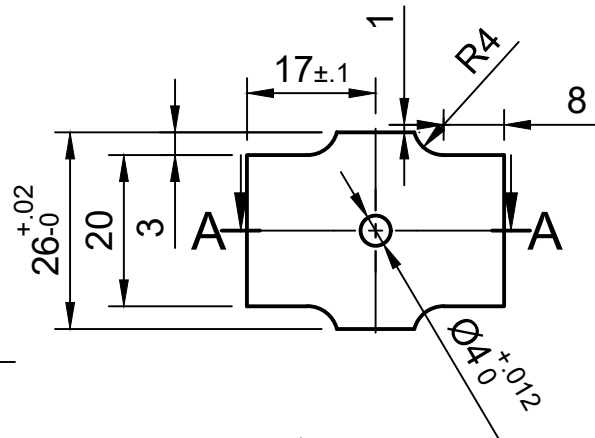
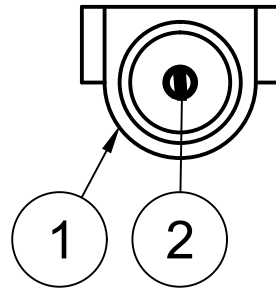
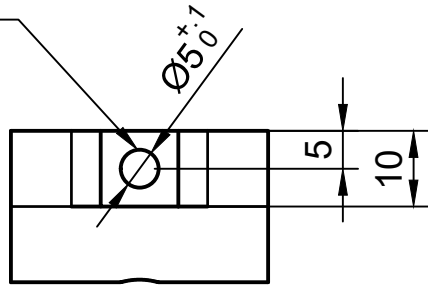


B-B (1:1)

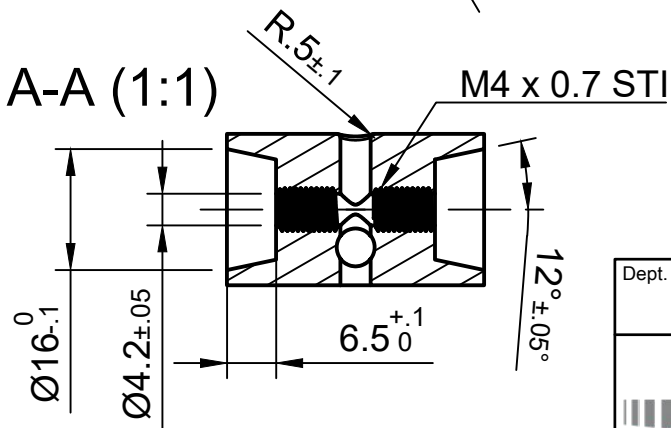


|       |                     |                           |                 |             |  |
|-------|---------------------|---------------------------|-----------------|-------------|--|
| Dept. | Technical reference | Created by<br>Ott Tahk    | 20.05.2019      | Approved by |  |
|       |                     | Document type             | Document status |             |  |
|       |                     | Title<br>TeeteringBracket | DWG No.         |             |  |
| Rev.  | Date of issue       | Sheet                     |                 | 1/1         |  |

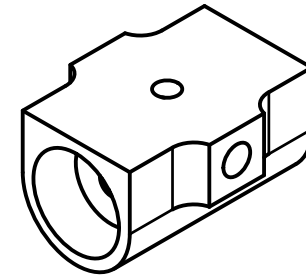
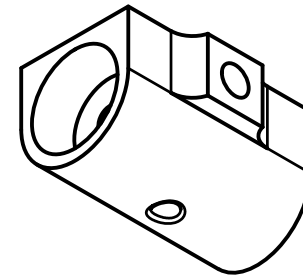
Through hole



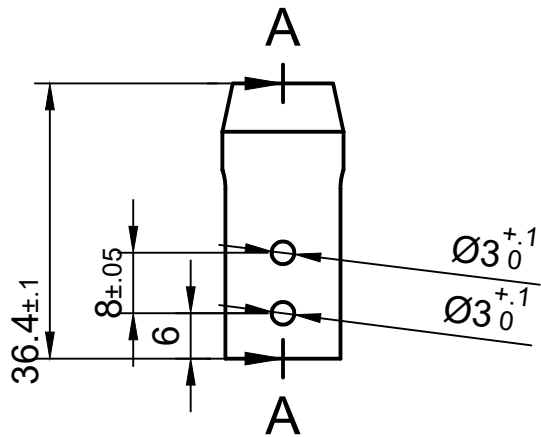
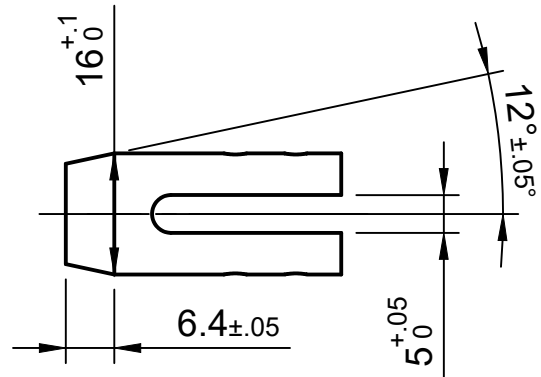
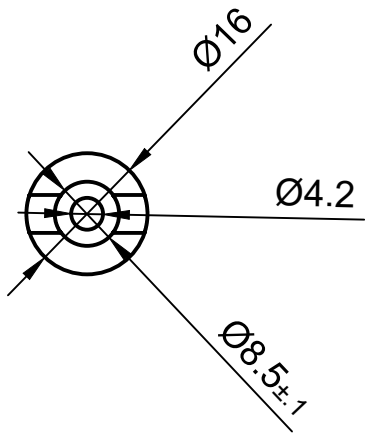
A-A (1:1)



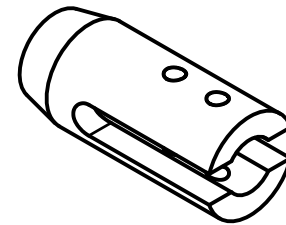
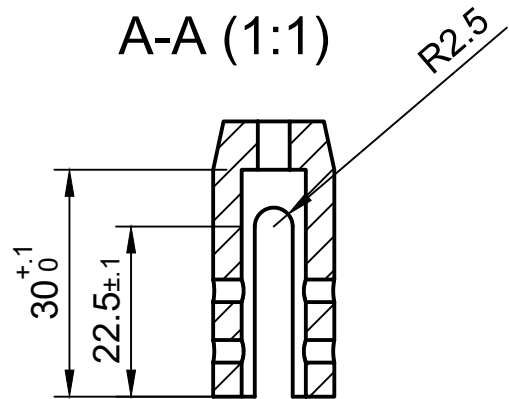
| Parts List |     |                       |                     |
|------------|-----|-----------------------|---------------------|
| Item       | Qty | Part Number           | Material            |
| 1          | 1   | Rotor_Hub v6          | Aluminum 6082 T6    |
| 2          | 2   | Threaded_Insert _M4x8 | Stainless Steel 304 |



|   |                     |                               |                 |             |  |
|---|---------------------|-------------------------------|-----------------|-------------|--|
| Dept.   | Technical reference | Created by<br><b>Ott Tahk</b> | 20.05.2019      | Approved by |  |
|  <b>TTÜ</b><br>DEPARTMENT OF MECHANICAL AND INDUSTRIAL ENGINEERING |                     | Document type                 | Document status |             |  |
|   |                     | Title<br><b>Rotor_Hub</b>     | DWG No.         |             |  |
| Rev.  | Date of issue       | Sheet                         |                 | 1/1         |  |

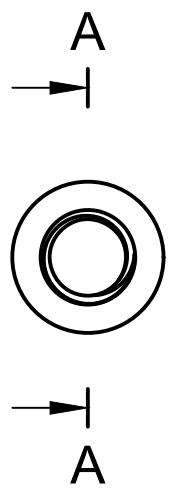


A-A (1:1)



|  |                     |                               |                 |                     |  |
|--|---------------------|-------------------------------|-----------------|---------------------|--|
| Dept.  | Technical reference | Created by<br><b>Ott Tahk</b> | 20.05.2019      | Approved by         |  |
|  <b>TTÜ</b><br>DEPARTMENT OF MECHANICAL<br>AND INDUSTRIAL ENGINEERING |                     | Document type                 | Document status |                     |  |
|  |                     | Title<br><b>Blade_Holder</b>  | DWG No.         |                     |  |
|  |                     | Rev.                          | Date of issue   | Sheet<br><b>1/1</b> |  |

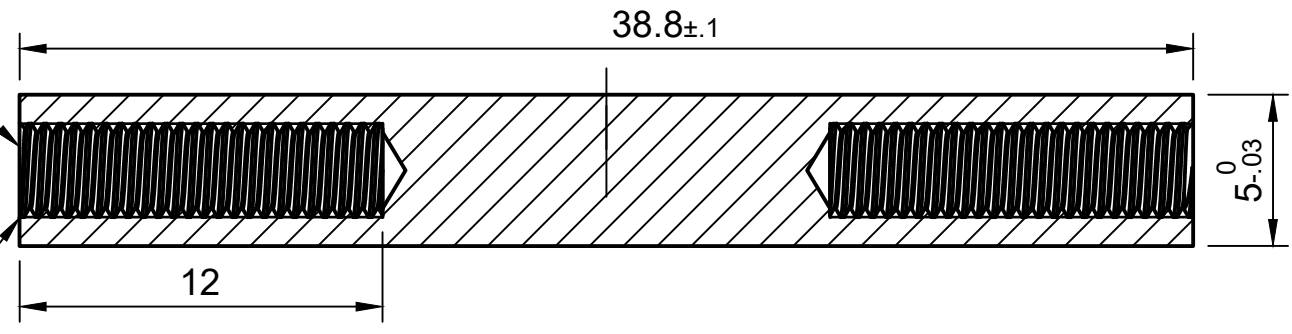




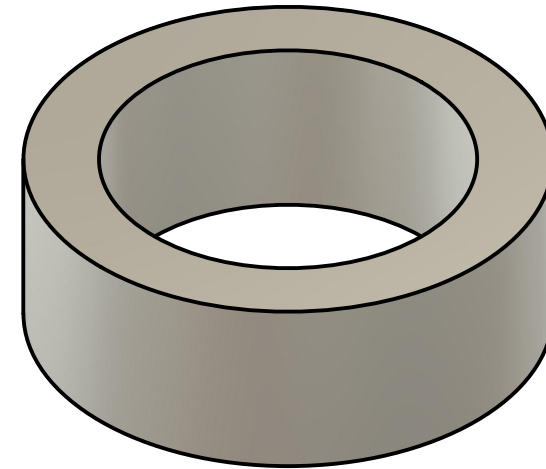
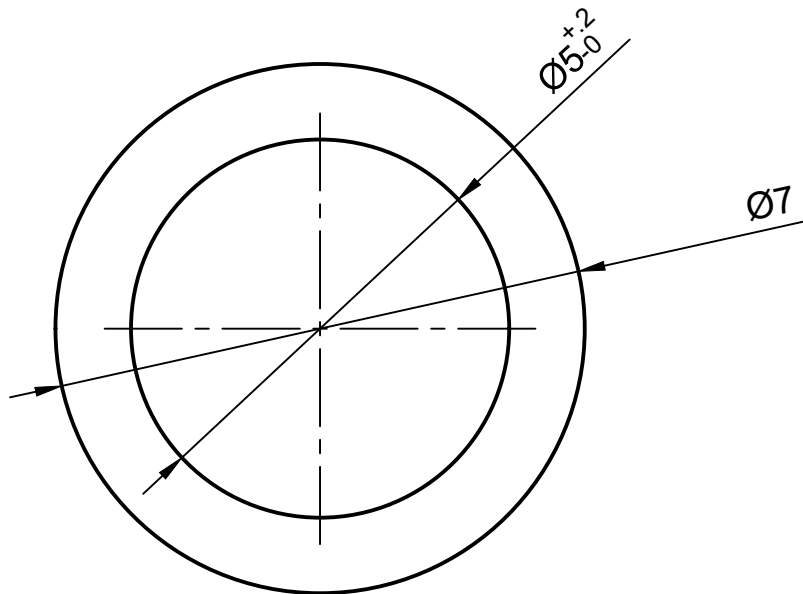
M3x0.5 6H  
Min L=9mm

chamfer at inlet  
45° 0.3mm

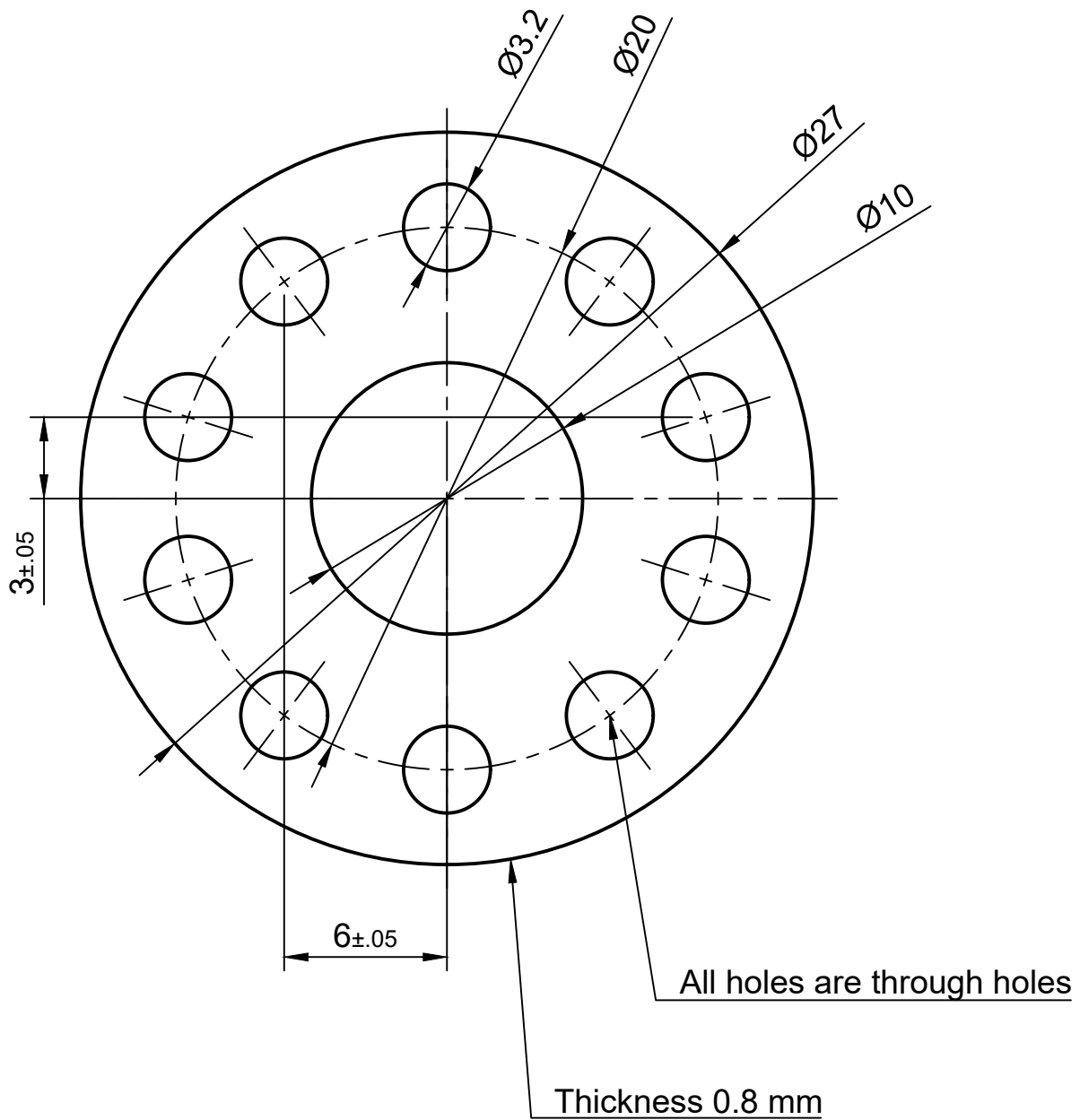
A-A (4:1)



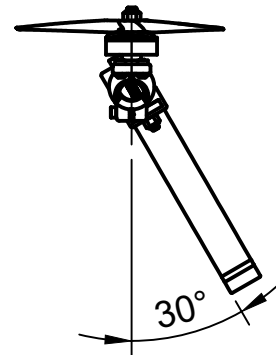
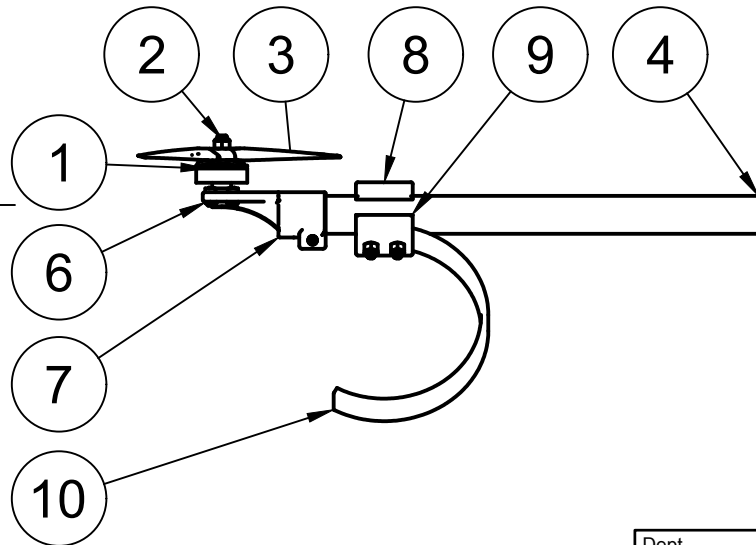
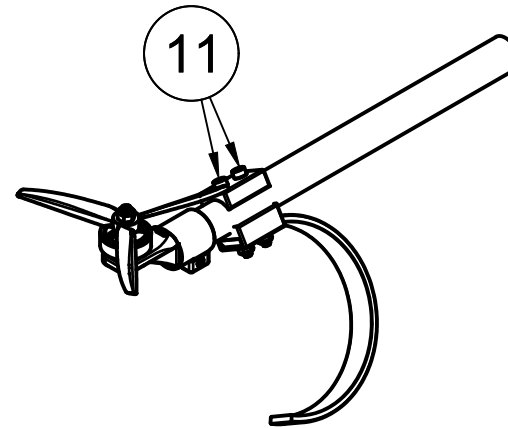
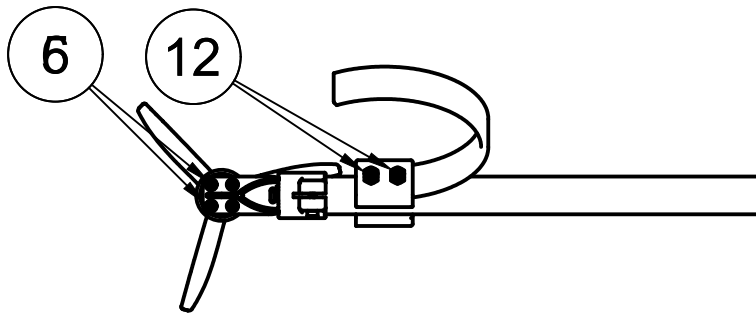
|  |                     |                               |                 |                     |  |
|--|---------------------|-------------------------------|-----------------|---------------------|--|
| Dept.  | Technical reference | Created by<br><b>Ott Tahk</b> | 20.05.2019      | Approved by         |  |
|  <b>TTÜ</b><br>DEPARTMENT OF MECHANICAL<br>AND INDUSTRIAL ENGINEERING |                     | Document type                 | Document status |                     |  |
|  |                     | Title<br><b>TeeterShaft</b>   | DWG No.         |                     |  |
|  |                     | Rev.                          | Date of issue   | Sheet<br><b>1/1</b> |  |



|  |                     |                                       |                 |                     |  |
|--|---------------------|---------------------------------------|-----------------|---------------------|--|
| Dept.  | Technical reference | Created by<br><b>Ott Tahk</b>         | 23.05.2019      | Approved by         |  |
|  <b>TTU</b><br>DEPARTMENT OF MECHANICAL<br>AND INDUSTRIAL ENGINEERING |                     | Document type                         | Document status |                     |  |
|  |                     | Title<br><b>Teeter_Spacer_5x2.5x7</b> | DWG No.         |                     |  |
|  |                     | Rev.                                  | Date of issue   | Sheet<br><b>1/1</b> |  |



|   |                     |   |                 |                     |             |
|---|---------------------|---|-----------------|---------------------|-------------|
| Dept.   | Technical reference | Created by<br><b>Ott Tahk</b>                                 | 20.05.2019      |                     | Approved by |
| <br><b>TTÜ</b><br>DEPARTMENT OF MECHANICAL<br>AND INDUSTRIAL ENGINEERING |                     | Document type   | Document status |                     |             |
|   |                     | Title<br><b>FacePlate</b><br><b>Material: Stainless steel</b> | DWG No.         |                     |             |
|   |                     | Rev.  | Date of issue   | Sheet<br><b>1/1</b> |             |

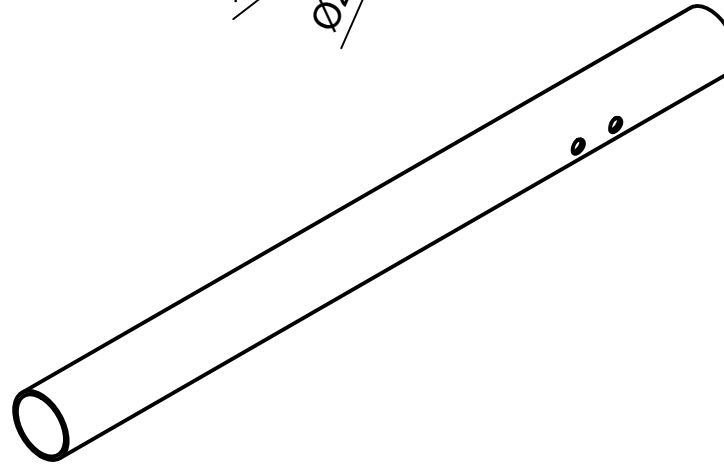
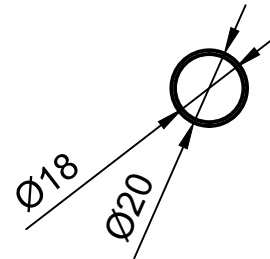
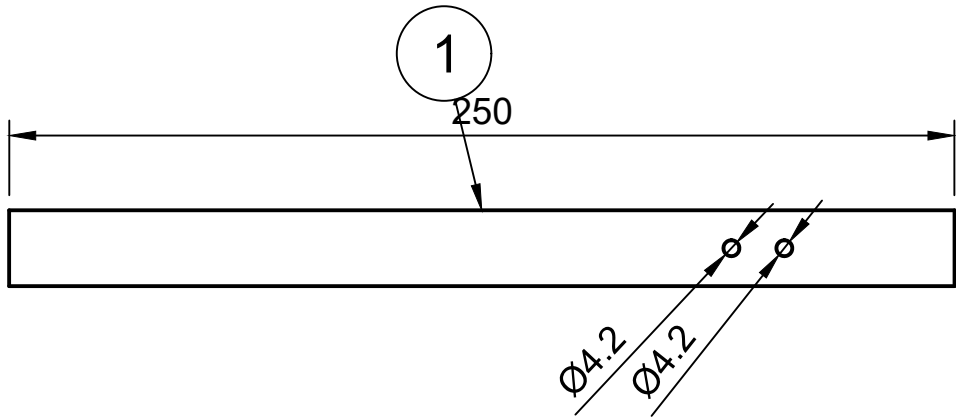


Parts List

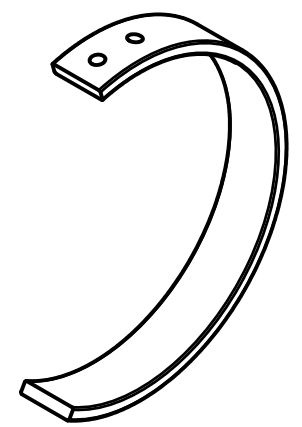
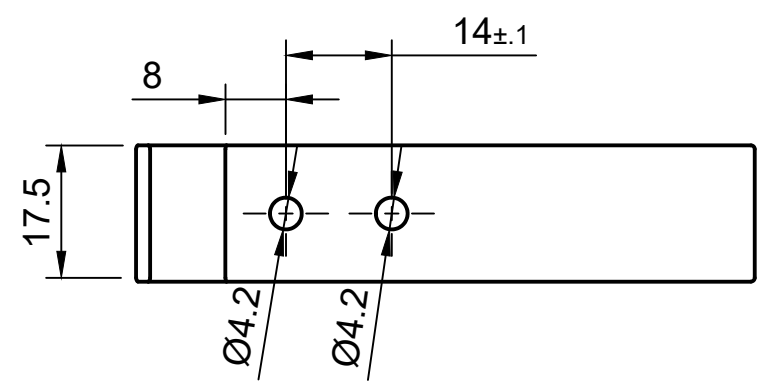
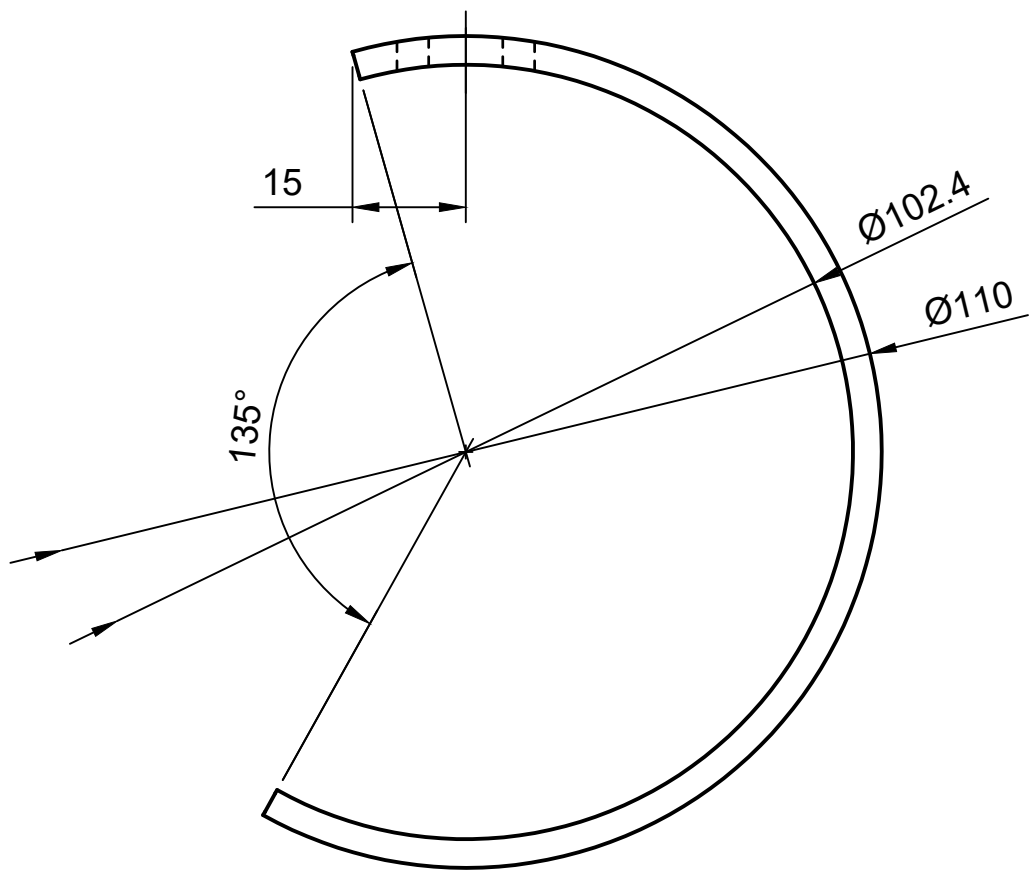
| Item | Qty | Part Number                         |
|------|-----|-------------------------------------|
| 1    | 1   | Motor_Hobbywing_RacePro_2207_1750KV |
| 2    | 1   | Nut_M5_Locking_Nylon                |
| 3    | 1   | Propeller_5_Inch                    |
| 4    | 1   | Boom                                |
| 5    | 4   | Bolt_M3x8_RoundHead_Hex             |
| 6    | 4   | Washer_M3_BrassFinish               |
| 7    | 1   | Mount_Boom_Motor                    |
| 8    | 1   | Landing_Gear_Bracket_Upper          |
| 9    | 1   | Landing_Gear_Bracket_Lower          |
| 10   | 1   | PP_110x18_Section                   |
| 11   | 2   | Bolt_M4x40                          |
| 12   | 2   | Nut_M4_Locking_Nylon                |

|       |                     |                               |                 |                     |
|-------|---------------------|-------------------------------|-----------------|---------------------|
| Dept. | Technical reference | Created by<br><b>Ott Tahk</b> | 22.05.2019      | Approved by         |
|       |                     | Document type                 | Document status |                     |
|       |                     | Title<br><b>BoomMotorAssy</b> | DWG No.         |                     |
|       |                     | Rev.                          | Date of issue   | Sheet<br><b>1/1</b> |

| Parts List  |                     |
|-------------|---------------------|
| Part Number | Material            |
| Boom        | Aluminum<br>6063 T6 |

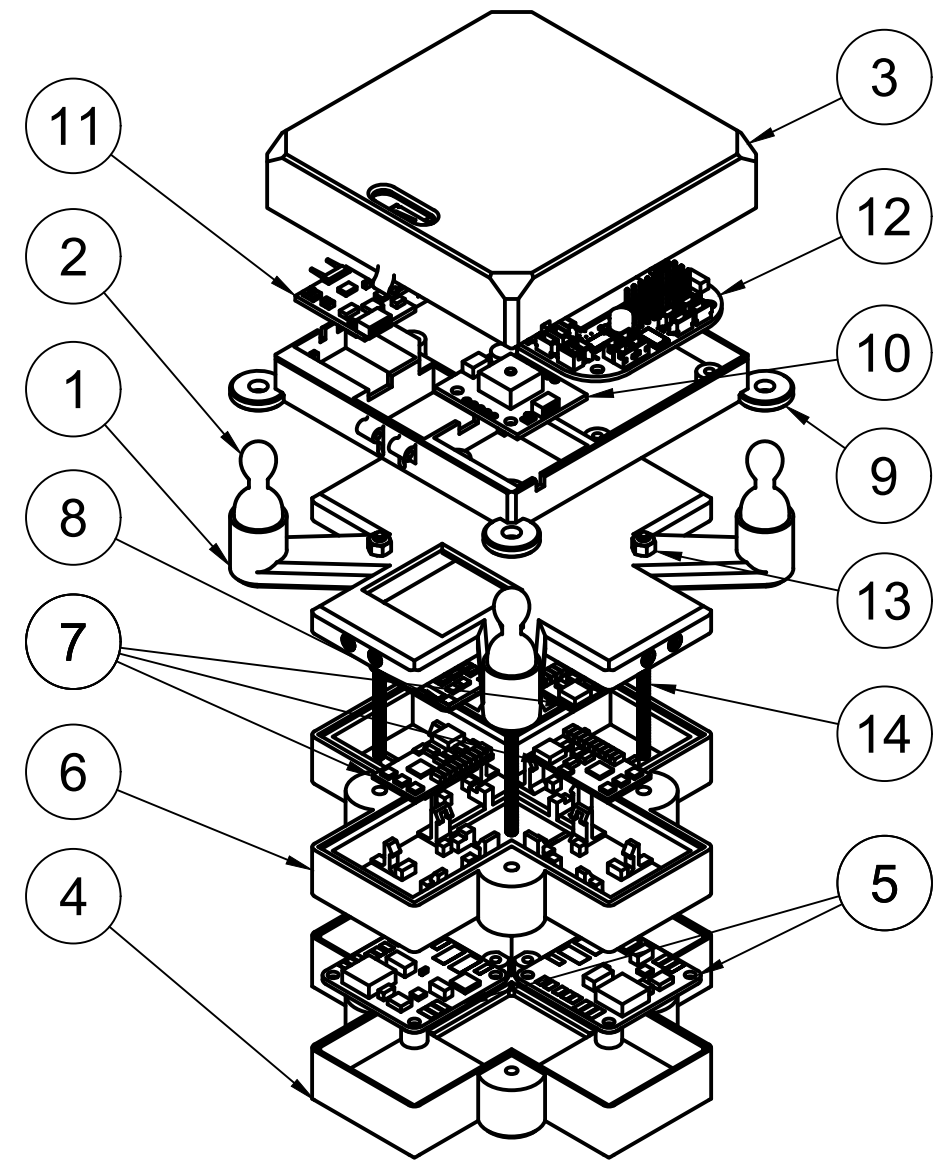
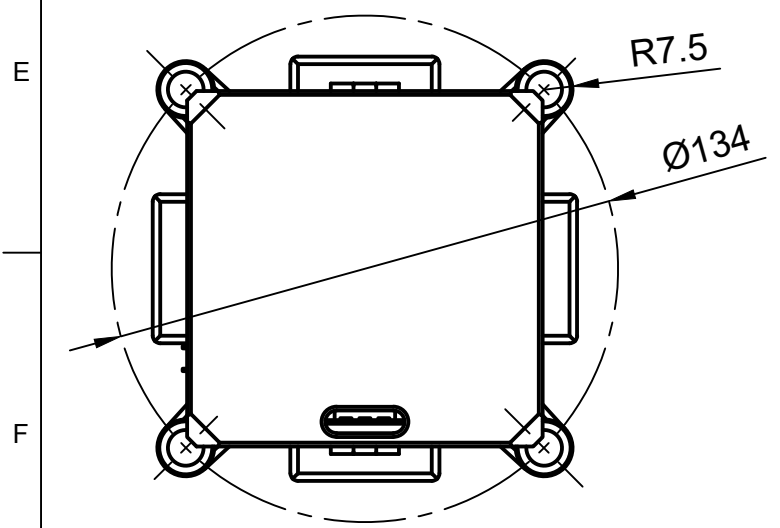
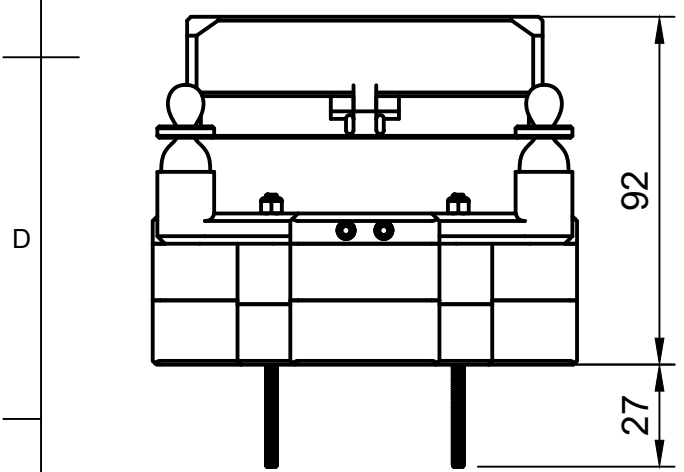
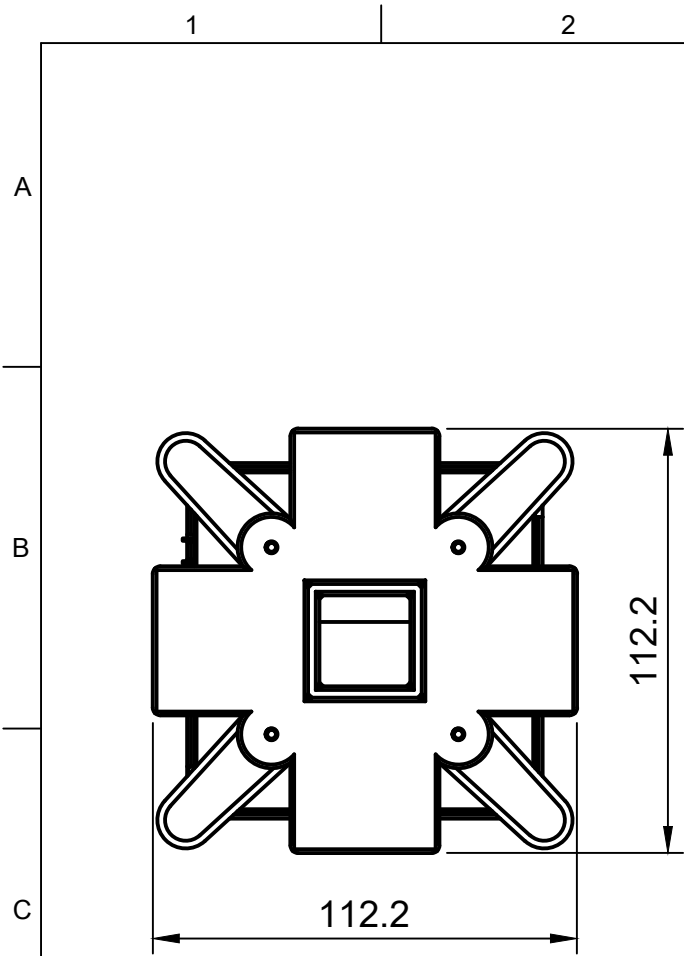


|  |                     |                               |                 |                     |  |
|--|---------------------|-------------------------------|-----------------|---------------------|--|
| Dept.  | Technical reference | Created by<br><b>Ott Tahk</b> | 22.05.2019      | Approved by         |  |
|  <b>TTÜ</b><br>DEPARTMENT OF MECHANICAL<br>AND INDUSTRIAL ENGINEERING |                     | Document type                 | Document status |                     |  |
|  |                     | Title<br><b>Boom</b>          | DWG No.         |                     |  |
|  |                     | Rev.                          | Date of issue   | Sheet<br><b>1/1</b> |  |



Cut from standard 110 mm polypropylene sewage pipe

|   |                                   |                               |            |                 |             |
|---|-----------------------------------|-------------------------------|------------|-----------------|-------------|
| Dept.   | Technical reference               | Created by<br><b>Ott Tahk</b> | 22.05.2019 |                 | Approved by |
|  <b>TTÜ</b><br>DEPARTMENT OF MECHANICAL AND INDUSTRIAL ENGINEERING | Document type                     |                               |            | Document status |             |
|   | Title<br><b>PP_110x18_Section</b> |                               |            | DWG No.         |             |
|   | Rev.                              | Date of issue                 |            | Sheet           | 1/1         |



| Parts List |     |                                   |                          |
|------------|-----|-----------------------------------|--------------------------|
| Item       | Qty | Part Number                       | Material                 |
| 1          | 1   | ESC_Cover                         |                          |
| 2          | 4   | Ear_Plug                          | Polyurethane Foam        |
| 3          | 1   | FlightControl_Box_Cover           | PLA_3D                   |
| 4          | 1   | Power_Distro_Box                  | PLA_3D                   |
| 5          | 4   | PowerDistroBoard_BabyPDB          |                          |
| 6          | 1   | ESC_Box                           | PLA_3D                   |
| 7          | 3   | ESC_Aikon                         |                          |
| 8          | 1   | ESC_Fav_CldPhnx_BLHeli32          |                          |
| 9          | 1   | FlightControl_Box                 | PLA_3D                   |
| 10         | 1   | GPS_Sparkfun_Qwiic                |                          |
| 11         | 1   | RC_Receiver                       |                          |
| 12         | 1   | Flight_Controller_BeagleBone_Blue | Various FlightController |
| 13         | 4   | Nut_M3_Locking_Nylon              |                          |
| 14         | 4   | Threaded_Rod_M3x72                | Steel                    |

|  |                     |                                      |                 |             |
|--|---------------------|--------------------------------------|-----------------|-------------|
| Dept.  | Technical reference | Created by<br><b>Ott Tahk</b>        | 23.05.2019      | Approved by |
| <br>DEPARTMENT OF MECHANICAL AND INDUSTRIAL ENGINEERING |                     | Document type                        | Document status |             |
|  |                     | Title<br><b>ElectronicsStackAssy</b> | DWG No.         |             |
| Rev.   | Date of issue       | Sheet<br><b>2/2</b>                  |                 |             |